

LOCKHEED MARTIN ENERGY RESEARCH LIBRARIES



LOCKHEED MARTIN LIBRARY
CURRENT COLLECTION

3 4456 0515948 6

ORNL-4097
UC-25 - Metals, Ceramics, and Materials

RADIATION METALLURGY SECTION

SOLID STATE DIVISION

PROGRESS REPORT

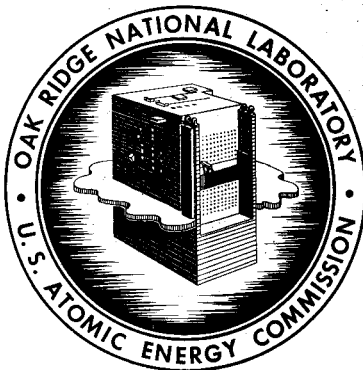
FOR PERIOD ENDING JANUARY 1967

CENTRAL RESEARCH LIBRARY
DOCUMENT COLLECTION

LIBRARY LOAN COPY

DO NOT TRANSFER TO ANOTHER PERSON

If you wish someone else to see this
document, send in name with document
and the library will arrange a loan.



OAK RIDGE NATIONAL LABORATORY

operated by

UNION CARBIDE CORPORATION

for the

U.S. ATOMIC ENERGY COMMISSION

Printed in the United States of America. Available from Clearinghouse for Federal
Scientific and Technical Information, National Bureau of Standards,
U.S. Department of Commerce, Springfield, Virginia 22151
Price: Printed Copy \$3.00; Microfiche \$0.65

LEGAL NOTICE

This report was prepared as an account of Government sponsored work. Neither the United States, nor the Commission, nor any person acting on behalf of the Commission:

- A. Makes any warranty or representation, expressed or implied, with respect to the accuracy, completeness, or usefulness of the information contained in this report, or that the use of any information, apparatus, method, or process disclosed in this report may not infringe privately owned rights; or
- B. Assumes any liabilities with respect to the use of, or for damages resulting from the use of any information, apparatus, method, or process disclosed in this report.

As used in the above, "person acting on behalf of the Commission" includes any employee or contractor of the Commission, or employee of such contractor, to the extent that such employee or contractor of the Commission, or employee of such contractor prepares, disseminates, or provides access to, any information pursuant to his employment or contract with the Commission, or his employment with such contractor.

ORNL-4097

Contract No. W-7405-eng-26

RADIATION METALLURGY SECTION
SOLID STATE DIVISION
PROGRESS REPORT
For Period Ending January 1967

D. S. Billington, Director, Solid State Division
M. S. Wechsler, Head, Radiation Metallurgy Section

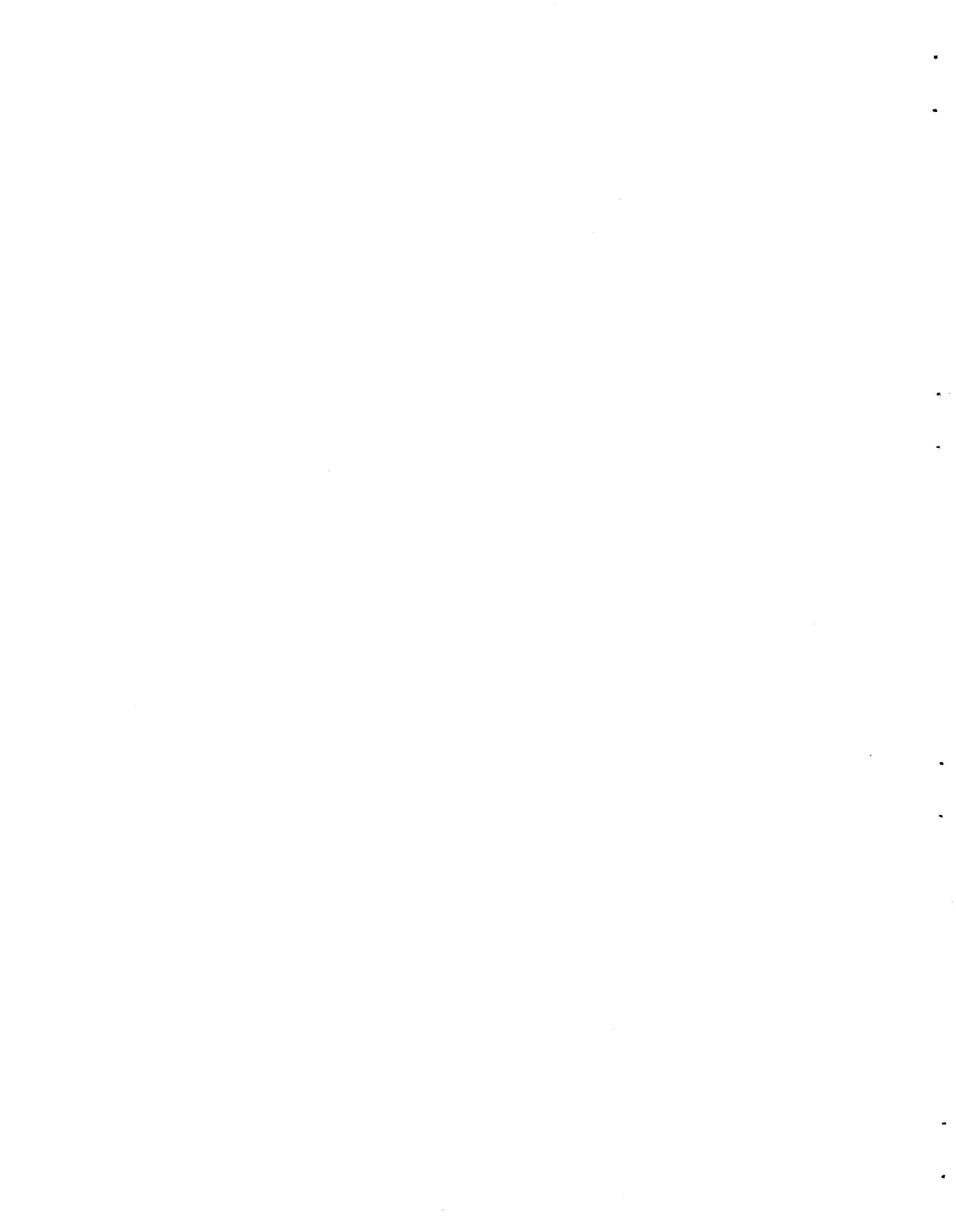
APRIL 1967

OAK RIDGE NATIONAL LABORATORY
Oak Ridge, Tennessee
Operated by
UNION CARBIDE CORPORATION
for the
U. S. ATOMIC ENERGY COMMISSION

LOCKHEED MARTIN ENERGY RESEARCH LIBRARIES



3 4456 0515948 6



Summary.....v

Radiation Metallurgy.....1

 Radiation Effects on Pressure-Vessel Steels.....1

 Tensile Tests on Irradiated Iron.....7

 On the Temperature and Strain Rate Dependence of Radiation Hardening
 in Iron.....13

 Niobium: Purification and Perfection.....20

 Purification.....20

 Perfection.....23

 Concerning the Etching of Dislocations in Niobium.....26

 The Interaction of Radiation Produced Defects and Interstitial
 Impurity Atoms in Niobium.....30

 Specimen Preparation.....32

 Measurement Techniques.....34

 Pre-Irradiation Measurements.....34

 Irradiation and Annealing Procedures.....36

 Internal Friction Results.....38

 Resistivity Results.....38

 Discussion.....40



SUMMARY

Studies of the radiation embrittlement of weld heat-affected-zone samples and base plate of ASTM A-212B pressure-vessel steel are continuing. In this report we show the effect of irradiation temperature on the shift of ductile brittle transition temperature of base plate and HAZ specimens of three different heats of A-212B steel. Heat to heat variations of sensitivity to radiation embrittlement are quite striking.

Studies of the increase of yield stress of ferrovac-E iron samples irradiated to the same dose but at different rates have now been completed. No effect of dose rate on yield stress increase was observed for dose rates ranging from about 1.7×10^{11} neutrons/cm² sec to 2.3×10^{13} neutrons/cm² sec ($E > 1$ Mev). Studies of annealing of radiation hardening were carried out in the temperature range from 300 to 400°C. It was observed that the radiation damage became more stable with increasing dose in the interval 4×10^{17} to 5×10^{18} neutrons/cm² ($E > 1$ Mev). Also the annealing did not take place with a constant activation energy. Studies were also carried out which indicate an effect of interstitial impurities in producing radiation hardening. In these studies samples were irradiated at low temperature and tested at 0°C with no apparent increase in yield stress. Similar samples given identical treatment but annealed in the temperature interval from 0 - 100°C before testing at 0°C, showed an increase in yield stress about equal to that observed in specimens irradiated at 90°C.

The temperature and strain rate dependence of the flow stress of irradiated polycrystalline iron specimens was tested. The results were analyzed to give activation energies and activation volumes for flow. The activation volume was not changed by irradiation while the activation energy was increased by irradiation.

A niobium single crystal with a total impurity content of < 75 ppm and a resistivity ratio $R_{300}/R_{4.2} = 1420$ was produced. An annealing procedure for improving the perfection of niobium single crystals was determined and x-ray topographs of the resulting crystals were made.

Studies of dislocation motion in niobium single crystals using etch pits were continued and procedures for decorating dislocations in very high purity niobium were determined.

Stage III annealing in irradiated niobium was studied using internal friction measurements and resistivity measurements. The results showed that Stage III annealing is due to migration of oxygen atoms to radiation produced defects. This result has important implications for theories of radiation hardening since it is known that a large hardness increase occurs during this annealing stage.

RADIATION METALLURGY

D. S. Billington, M. S. Wechsler, and J. T. Stanley

The major emphasis of research in the Radiation Metallurgy Section is the study of radiation-hardening and radiation embrittlement in the bcc metals and alloys. These metals have in common the tendency toward low-temperature brittleness which can be characterized by the ductile brittle transition temperature. The increase in ductile-brittle transition temperature upon irradiation is of concern in reactor technology because of the possible catastrophic failure of reactor pressure vessels in service. The work described in this report shows the influence of metallurgical variables, i.e. internal structure such as grain boundaries and distribution of various phases as determined by heat treatment, in determining the response of a steel to irradiation hardening. Of course this is a very complex problem and in order to study certain aspects it is necessary to work with somewhat simpler systems than pressure vessel steel. High purity iron polycrystalline specimens and high purity niobium single crystals are being used to study dislocation motion and interaction with radiation produced defects. Since the interaction of interstitial impurities with radiation produced defects may play an important role in radiation hardening mechanisms, studies of these interactions are being made.

Radiation Effects on Pressure-Vessel Steels

R. G. Berggren W. J. Stelzman
T. N. Jones

We have previously reported on the effect of fast neutron dose and irradiation temperature on the Charpy V-notch transition temperature of three heats of ASTM A-212 Grade B base plate and synthetic heat-affected

zone samples.^{1,2} Additional ductile-brittle transition temperature data have been obtained; these, with the previous data, are presented in Table 1.

In the unirradiated condition, the particular weld thermal cycles and stress relief imposed upon these three heats of A-212B steel increased the ductile-brittle transition temperatures. The largest increase (SSD Item 147-HAZ - 2B) has been attributed to the presence of continuous networks of proeutectoid ferrite at prior austenite grain boundaries.^{3,4} Comparison of the irradiated base plate and heat-affected zone specimens for each of the three heats at a 60 to 74°C irradiation temperature and a dose range of 8 to 10 x 10¹⁸ neutrons/cm² (E > 1 Mev) indicates that the sensitivity of each condition to irradiation is related to the cooling rate encountered in each thermal cycle. When one considers that the base plates have the slowest cooling rates, then the samples from all three heats with the highest cooling rates showed the least shift in transition temperature and the slowest cooling rates (normalized base plates) the highest shift. Similar behavior has been noted by Carpenter, Knopf, and Byron.⁵

Normalization of these data to a dose of 9 x 10¹⁸ neutrons/cm² (E > 1 Mev) following the trend band for A-212B irradiations yields the change in transition temperature at the 20 ft. lb. energy level for various

¹R. G. Berggren, W. J. Stelzman, and T. N. Jones, "Radiation Effects on Pressure-Vessel Steels," Radiation Metallurgy Section Solid State Division Progress Report, February, 1966, ORNL-3949, p. 2.

²R. G. Berggren, W. J. Stelzman, and T. N. Jones, "Radiation Effects on Pressure-Vessel Steels," Radiation Metallurgy Section Solid State Division Progress Report, July, 1966, ORNL-4020, p. 1.

³E. F. Nippes, W. F. Savage, and W. A. Brown, "Study of the Weld Heat-Affected Zone of A-212B Steel," Rensselaer Polytechnic Institute, Troy, N. Y. (February 1961).

⁴W. F. Savage and F. C. Breimeister, "A Further Study of the Weld Heat-Affected Zone in A-212B Steel," Rensselaer Polytechnic Institute, Troy, N. Y. (January 1964).

⁵G. F. Carpenter, N. R. Knopf, and E. S. Byron, "Anomalous Embrittling Effects Observed During Irradiation Studies on Pressure Vessel Steels," Nuclear Science and Engineering 19, 18-38, (1964).

Table 1 (Continued)

SSD Item No.	147	147	147	156	156	156	157	157	157
Thermal Cycle	None	4B	2B	None	2	3	None	2	3
Cooling Rate at 538°C	24.4°C/Sec	7.8°C/Sec	12.2°C/Sec	5.2°C/Sec	12.2°C/Sec	5.2°C/Sec	12.2°C/Sec	5.2°C/Sec	
Irradiation									
Temp. (°C)	Dose (E > 1 Mev)		DBTT at 20 ft-lb, (°C)						
	(x 10 ¹⁸ n/cm ²)								
260	9.6								132
277-283	7	18		62					
"	8			62					
"	11						55		
288-291	9				75			98	
"	10-10.3			72		70	63		107
321	9			72					
333	8	2							
337	7	20							
340	9-10	10	9	70					
360	10		-5				23		
440	8				2				
471	10	3							
474	9					15			

7

irradiation temperatures shown in Figs. 1 to 4. A comparison shows that the effects of irradiations vary considerably for the three heats and, for the case in hand, show that it is minimized in heat A-2056 (SSD Item 157) for both the base plate and heat-affected zone specimens. Not enough is known of the normalization histories of these heats to reach any conclusions regarding the difference in irradiation sensitivities.

It is also apparent that for the high temperature irradiation, there is little or no decrease or "recovery" of the transition temperature in the irradiation temperature range up to 250°C; however, recovery of the major portion of irradiation-induced transition temperature shifts for all conditions occurs within a fairly narrow band of less than 100°C (260 to 350°C), leaving 10% or less of the original damage remaining.

A cursory comparison of the high temperature irradiations with the post irradiation heat treatment data presented previously^{1,2} indicates that a heat treatment of 1 2/3 to 3 hrs. may afford as much recovery as the high temperature irradiations at the same temperature. Further post irradiation recovery studies are planned on materials already irradiated.

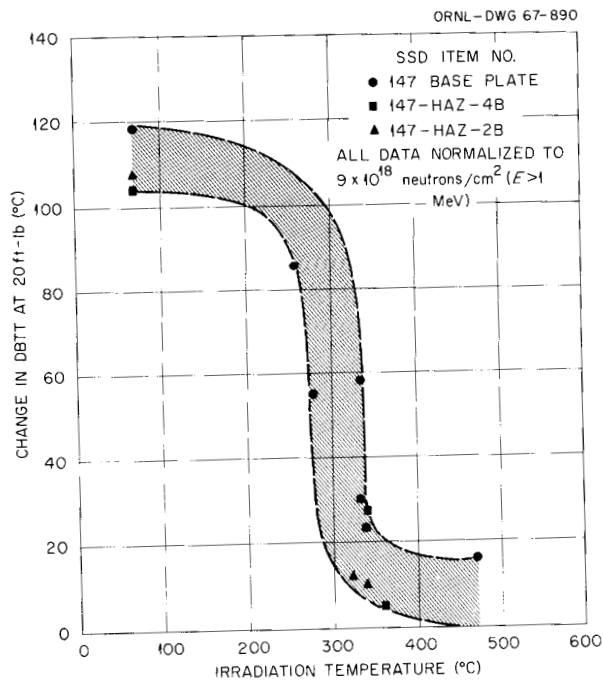


Fig. 1. Change in Charpy V-Notch Transition Temperature for Heat 15900 (SSD Item 147) of ASTM-A212-B Steel.

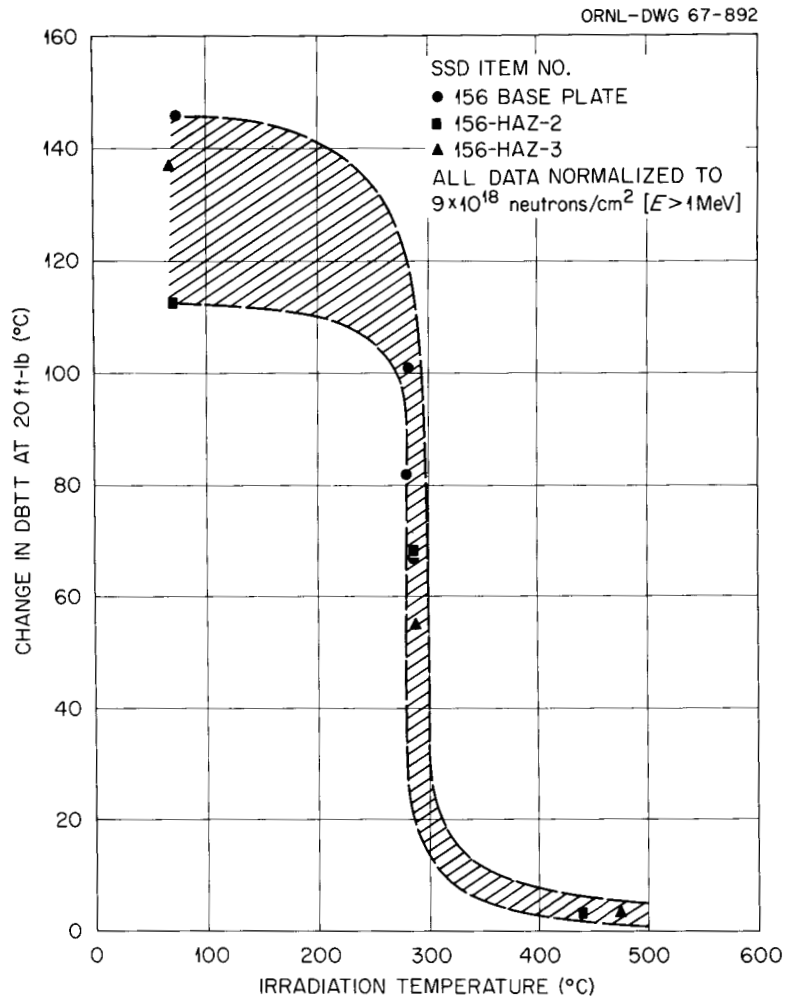


Fig. 2. Change in Charpy V-Notch Transition Temperature for Heat A-2110 (SSD Item 156) of ASTM A-212-B Steel.

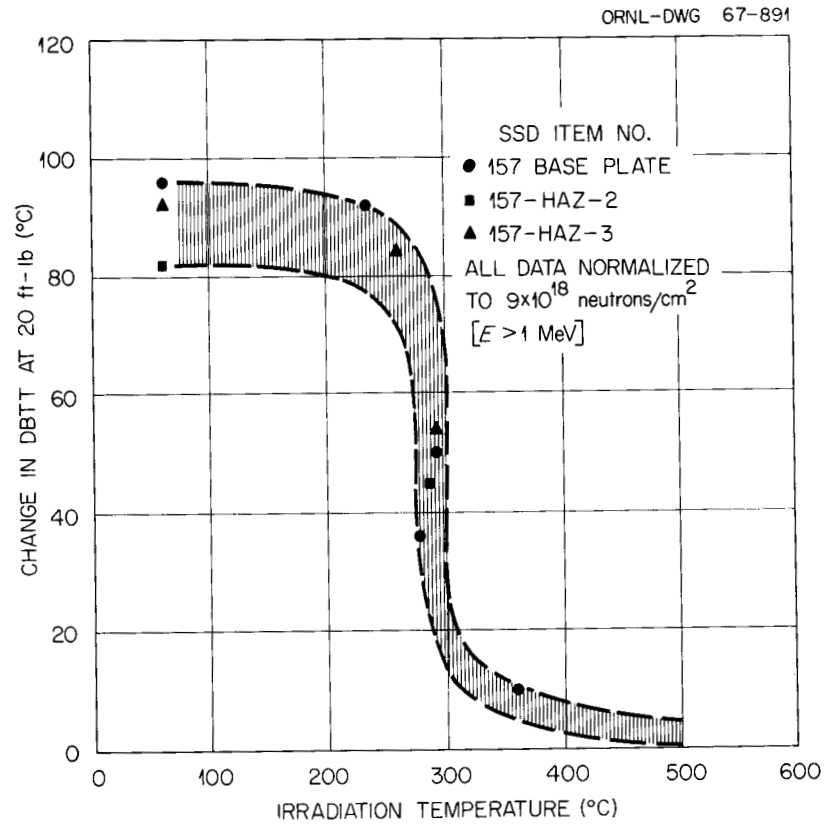


Fig. 3. Change in Charpy V-Notch Transition Temperature for Heat A-2056 (SSD Item 157) of ASTM A-212-B Steel.

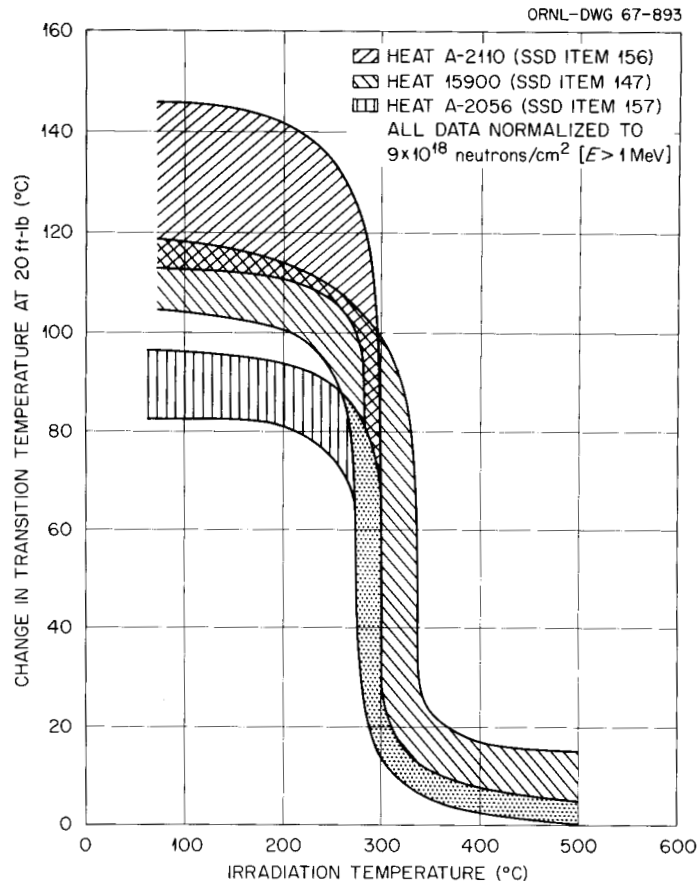


Fig. 4. Change in Charpy V-Notch Transition Temperature for Three Heats of ASTM A-212-B Steel. Both Base Plate and Synthetic Heat-Affected Zone Specimens.

Tensile Tests on Irradiated Iron

N. E. Hinkle N. K. Smith

The effect of neutron dose rate on the tensile properties of a high purity vacuum-melted iron (Ferrovac-E) has been studied. The importance of understanding the effect of dose rate may be realized when it is pointed out that materials irradiations are performed in research reactors having neutron dose rates of 10^{12} to 5×10^{13} neutrons/cm² · sec ($E > 1$ Mev) whereas the structural material of the pressure vessel of a power reactor is subjected to dose rates of 10^9 to 10^{11} neutrons/cm² · sec ($E > 1$ Mev).⁶

⁶J. J. DiNunno and A. B. Holt, "Radiation Embrittlement of Reactor Vessels," Nuclear Safety 4, 34 (1962).

The experimental details of the irradiations and some preliminary results have been described in previous reports of this series.⁷⁻⁹ To briefly summarize, tensile samples of Ferrovac-E iron, vacuum annealed and furnace cooled to obtain a grain size of 130μ , were irradiated to a dose of about 5×10^{18} neutrons/cm² ($E > 1$ Mev) in experiment assemblies located at increasing distances from the Oak Ridge Research Reactor. The irradiation temperature was 95° C and the neutron dose rates ranged from about 2×10^{11} to 2×10^{13} neutrons/cm² · sec ($E > 1$ Mev). Tensile testing of as-irradiated samples from each assembly has been completed. The results of this study, as shown in Fig. 5, indicate that there is no dose rate effect within the range of dose rates used at the neutron dose of 5×10^{18} neutrons/cm².

⁷N. E. Hinkle and N. K. Smith, "Tensile Tests on Irradiated Iron," Quarterly Progress Report: Irradiation Effects on Reactor Structural Materials, May, June, July, 1965, BNWL-218, pp. 10.25-10.35, August, 1965.

⁸N. E. Hinkle, N. K. Smith, and M. S. Wechsler, "Tensile Tests on Irradiated Iron," Quarterly Progress Report: Irradiation Effects on Reactor Structural Materials, November, December, 1965, January, 1966, BNWL-CC-510, pp. 10.8-10.27, February, 1966.

⁹N. E. Hinkle and N. K. Smith, "Tensile Tests on Irradiated Iron and Iron Alloys," Quarterly Progress Report: Irradiation Effects on Reactor Structural Materials, November, December, 1964, January 1965, HW-84618, pp. 10.31-10.43, February 15, 1965.

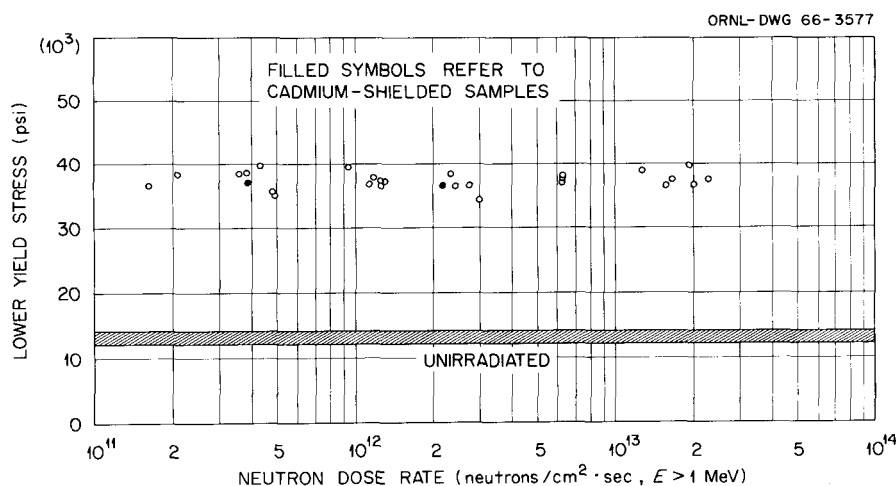


Fig. 5. Lower Yield Stress vs Dose Rate for Ferrovac-E Iron. Grain Size, 130 Microns. Irradiation Dose and Temperature, 4.6×10^{18} neutrons/cm² ($E > 1$ Mev) at 95° C. Test Temperature 30° C.

Post-irradiation annealing has been performed on samples irradiated at about 95°C to neutron doses of 4.5×10^{17} to 5×10^{18} neutrons/cm² ($E > 1$ Mev). The results are shown in Figs. 6, 7, and 8 as percent recovery vs annealing time at indicated annealing temperature. In Fig. 6 the different slopes for the data at various annealing temperatures indicate damage recovery at the lowest dose does not occur by a unique recovery process. The annealing studies on samples irradiated to a slightly greater dose, as shown in Fig. 7, appear to support the viewpoint that the damage recovery is not singly activated. Bryner¹⁰ has presented evidence from studies of post-irradiation annealing of Ferrovac-E that indicate that more than one thermally activated process is responsible for the damage recovery in iron. The data in Fig. 8 for the highest neutron dose show that for a given annealing time, the recovery percentage decreases with increasing dose. This is especially true for

¹⁰J. S. Bryner, "Electron-Transmission Microscope Study of Defects in Neutron Irradiated Iron," Quarterly Progress Report: Irradiation Effects on Reactor Structural Materials, May, June, July, 1966, BNWL-CC-784, pp. 5.1-5.3, August, 1966.

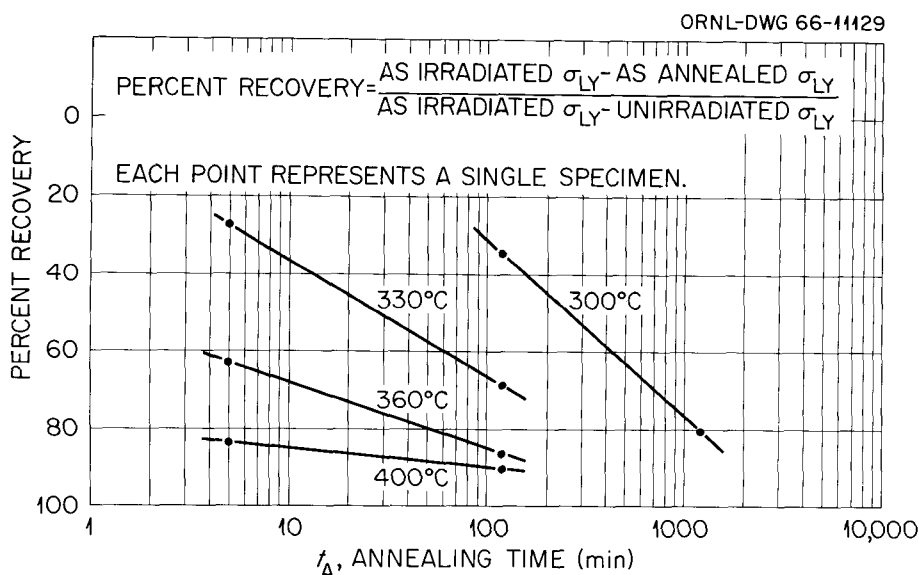


Fig. 6. The Percent Recovery of Radiation Induced Strengthening by Post Irradiation Annealing at the Given Temperatures. Test Temperature = 30°C. Strain Rate = 0.02 min⁻¹. Neutron Flux = 2×10^{12} to 2.9×10^{12} n/cm² · sec ($E > 1$ Mev). Neutron Dose = 4.5×10^{17} to 6.4×10^{17} n/cm² ($E > 1$ Mev).

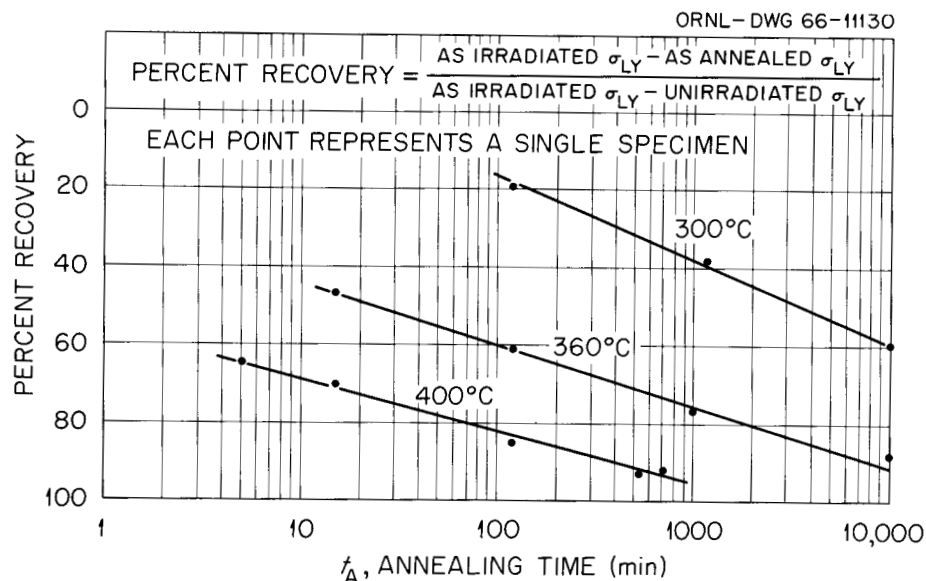


Fig. 7. The Percent Recovery of Radiation Induced Strengthening by Post Irradiation Annealing at the Given Temperatures. Test Temperature = 30°C. Strain Rate = 0.02 min⁻¹. Neutron Flux = (3.1 to 6.2) × 10¹² n/cm² · sec (E > 1 Mev). Neutron Dose = (6.8 to 13.7) × 10¹⁷ n/cm² (E > 1 Mev).

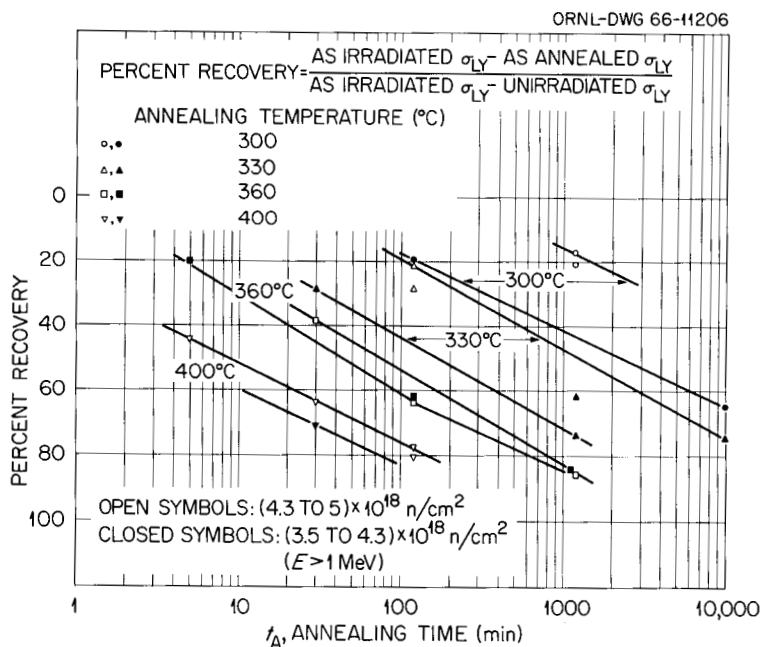


Fig. 8. The Percent Recovery of Radiation Induced Strengthening by Post Irradiation Annealing at the Given Temperatures. Test Temperature = 30°C. Strain Rate = 0.02 min⁻¹. Neutron Flux = 1.7 × 10¹¹ to 2.25 × 10¹³ n/cm² · sec (E > 1 Mev). Neutron Dose = (3.5 to 5) × 10¹⁸ n/cm² (E > 1 Mev).

annealing temperatures of 300° and 330°C. Additional testing has confirmed this trend. The apparent increased stability of the radiation damage with increasing neutron dose may be explained by the existence of two or more defect types having different activation energies for recovery and whose relative hardening effects change with increasing neutron dose. It is also likely that the relative effects of such defect types may be changed as a function of the irradiation temperature.

A possible explanation for the unusual damage recovery results presented above is that the interstitial impurities carbon, nitrogen, and oxygen, being mobile at the irradiation temperature of 95°C, may be combining with radiation induced defects to produce various defect arrangements each of which have a different hardening effect on the base material and different activation energy for recovery. As a first step toward resolving some of these problems, four vacuum annealed and furnace cooled tensile samples of 46 μ grain diameter Ferrovac-E were irradiated at -130°C in the Bulk Shielding Reactor (BSR) to a neutron dose of 7.8×10^{16} ($E > 1$ Mev). This irradiation temperature is well below the 0°C minimum predicted mobility temperature of any of these interstitial atoms. After irradiation, these samples were stored in liquid nitrogen before testing. In addition four identical samples were irradiated at about 90°C in a hydraulic tube in the Oak Ridge Research Reactor (ORR) to a dose of 1.25×10^{17} neutrons/cm² ($E > 1$ Mev). These samples and the controls were stored at room temperature before testing.

These samples were tested in an Instron tensile machine at a strain rate of 2% per minute and at a test temperature of 0°C at which the interstitials were not expected to be mobile. The results of the tests, shown in Fig. 9, indicate that only a small percentage of the damage accumulated in the irradiations at 90°C is attributable to the low temperature neutron bombardment and subsequent thermal rearrangements occurring below 0°C. It is also shown that a large part of the increased yield strength found after the irradiation at 90°C may be induced in the samples irradiated at very low temperatures by a 10 min. anneal at 100°C. Similar anneal hardening has been observed by Makin and Minter¹¹ in

¹¹M. J. Makin and F. J. Minter, "The Mechanical Properties of Irradiated Molybdenum," *Acta Met.* 7, pp. 361-366 (1959).

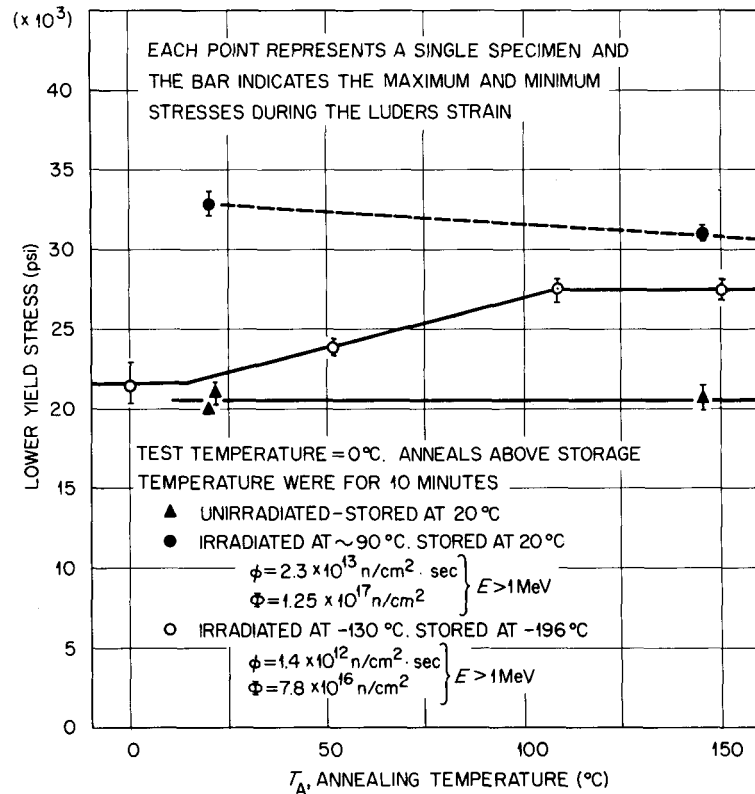


Fig. 9. Lower Yield Stress at 0°C as a Function of Irradiation Temperature and Post-Irradiation Annealing for Tensile Specimens of Vacuum-Melted Iron Vacuum Annealed at 815°C for 5 Hours and Furnace Cooled. Grain Diameter $\sim 4\mu$. Strain Rate = 0.02 min⁻¹.

niobium and by Moteff¹² and co-workers for tungsten and molybdenum. The interstitial content of the Ferrovac-E iron samples was not controlled; therefore, it is not possible to relate the anneal hardening to the presence or absence of certain interstitials. However, it is clear that some thermally activated rearrangement occurs between 0° and 100°C and it is believed that interaction of the interstitial elements with the radiation induced defects is responsible for the observed effect. More detailed experiments, using controlled additions of nitrogen and carbon to iron and sensitive physical techniques to detect the effects of the interstitial element mobility and activity, are in the preliminary stage and will be discussed fully in a future report.

¹²J. Moteff, "Radiation Damage in Body-Centered Cubic Metals and Alloys," in Radiation Effects in Materials, New York, Gordon and Breach, 1966.

The absence of a dose rate effect in our studies may be a result of the complications arising out of the interactions of the interstitial impurities with the radiation induced defects. Also, the wide variation in the dose dependence of the radiation damage previously reported in our studies may be ascribed to the same problem.

On The Temperature And Strain Rate Dependence Of
Radiation Hardening In Iron

S. M. Ohr

E. D. Bolling

The strong temperature and strain rate dependence of the yield and flow stresses of the body-centered-cubic metals indicates that the thermal activation of dislocation motion plays a significant role in the deformation process. Although the thermal activation of dislocation motion has been the subject of a number of investigations,^{13, 14} no attention has so far been given to neutron irradiated body-centered-cubic metals. An understanding of the rate processes as reflected by the strong temperature and strain rate dependence of the yield stress is of considerable interest because of the influence which these factors have on the ductile-brittle transition in the body-centered-cubic metals. In this report, a preliminary account of an investigation of the temperature and strain rate sensitivity of the yield stress of neutron irradiated and unirradiated Ferrovac-E iron is given.

Small tensile samples of 1/2-gage-length were prepared from cold rolled sheets of 0.01-in.-thickness. These samples were annealed in vacuo to achieve a uniform average grain diameter of approximately 30 μ . The tensile samples, shielded with cadmium, were irradiated at temperatures between 57° and 90°C in the poolside facility of the ORR at a dose rate of approximately 3×10^{12} neutrons/cm² sec. to a dose of 1.2×10^{16}

¹³H. Conrad, "Yielding and Flow of the B.C.C. Metals at Low Temperatures," p. 476 in The Relation Between the Structure and Mechanical Properties of Metals, Her Majesty's Stationery Office, London, 1963.

¹⁴H. Conrad, "On the Mechanism of Yielding and Flow in Iron," J. Iron and Steel Inst. 364, 198 (1961).

neutrons/cm² ($E > 1$ Mev). Tensile deformation was carried out at various temperatures in baths of liquid nitrogen (77°K), dry ice - acetone (195°K), Freon 12 (243°K), ice water (273°K), and at room temperature (298°K). In order to measure the strain rate sensitivity, the cross-head speed of the Instron tensile machine was cycled by an order of magnitude between the strain rates of $6.56 \times 10^{-5} \text{ sec}^{-1}$ and $6.56 \times 10^{-4} \text{ sec}^{-1}$. In some of the tests, a change in test temperature was made on a given sample to measure the temperature dependence of the yield stress at a constant dislocation configuration. In addition, stress relaxation tests were carried out at room temperature to determine accurately the athermal component of the yield stress, as well as to measure the rate sensitivity at small effective stresses.

Figure 10 shows the temperature dependence of the lower yield stress for unirradiated and irradiated iron, tested at a strain rate of $6.56 \times 10^{-5} \text{ sec}^{-1}$. The overall effect of neutron irradiation is an upward shift of the yield stress curve without an appreciable change in its shape. It may be noticed, however, that the gap between the two curves

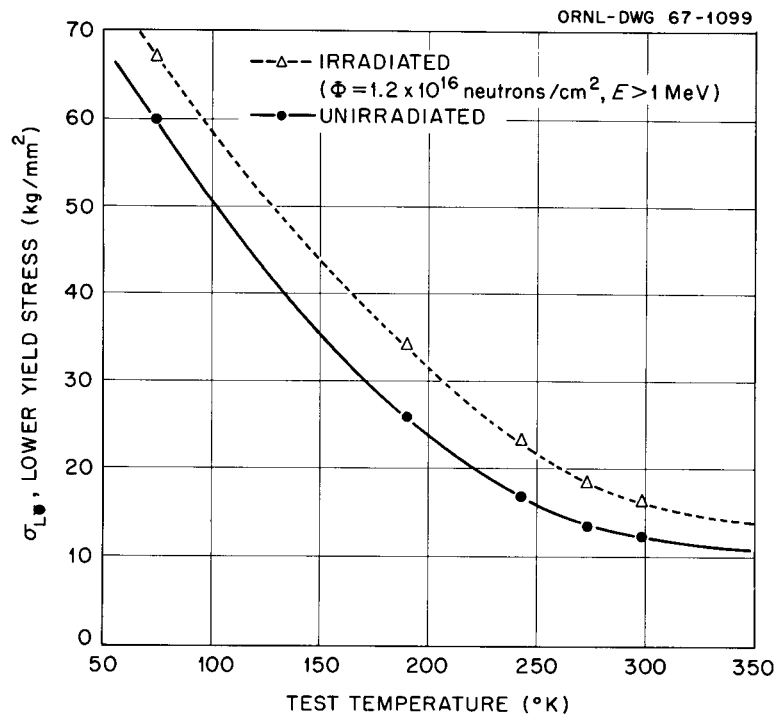


Fig. 10. Temperature Dependence of Lower Yield Stress for Unirradiated and Neutron Irradiated Polycrystalline Ferrovac-E Iron.

does gradually narrow as the temperature is increased. Thus neutron irradiation seems to have slightly modified the temperature dependence of the yield stress.

It is generally accepted that the yield stress consists of two components, namely thermal and athermal. It is the thermal component of the stress, or the effective stress, that varies with test temperature. The effective stress is a measure of the degree of thermal activation in overcoming the short range obstacles to dislocation motion. Also, it is the stress that is effective in moving dislocations. The athermal component defines the stress level that has to be supplied by the applied stress in overcoming the long range internal stress in the crystal. To determine the thermal component of yield stress, it is necessary to determine the athermal component and to subtract it from the applied stress. In earlier works,¹⁴ the athermal component has been taken as the yield stress at a sufficiently high temperature. Recently, Li¹⁵ has suggested a method of determining the internal stress from a stress relaxation test by utilizing equations governing dislocation dynamics. When his method is applied to the stress relaxation data, obtained from both unirradiated and irradiated samples, the stress dependence of dislocation velocity, m^* , is found to be approximately 4.0 and it is not affected by neutron irradiation. It is also found that the athermal component of the stress is increased by approximately 3.4 kg/mm^2 upon irradiation. This change can account for almost all of the increase in the yield stress at room temperature due to neutron irradiation. At low temperatures, the effective stress has also been increased by irradiation. This is shown in Figure 11 in which the effective stress is plotted as a function of temperature. This increase in the effective stress in irradiated samples may be due to either a difficulty in generating fresh dislocations, a

¹⁵J. C. M. Li, "Dislocation Dynamics in Deformation and Recovery," to be published in the Canadian Journal of Physics.

decrease in the effective gage length of the sample arising from dislocation channeling,^{16, 17} or a modification of the rate processes.

One of the parameters of interest in thermal activation analysis is the activation volume. The activation volume, v , represents the strain rate sensitivity of yield or flow stress, and it can be determined experimentally through the expression¹³

$$v = k T \left(\frac{\partial \ln \dot{\epsilon}}{\partial \tau} \right)_T \quad (1)$$

¹⁶B. Mastel, H. E. Kissinger, J. J. Laidler, and T. K. Bierlein, "Dislocation Channeling in Neutron Irradiated Molybdenum," J. Appl. Phys. 34, 3637 (1963).

¹⁷R. J. Arsenault, "The Possibility of Irradiation Damage Affecting the Rate-Controlling Mechanism for Slip in Body-Centered-Cubic Metals and Solid Solutions," ORNL Report No. 3993, 1966.

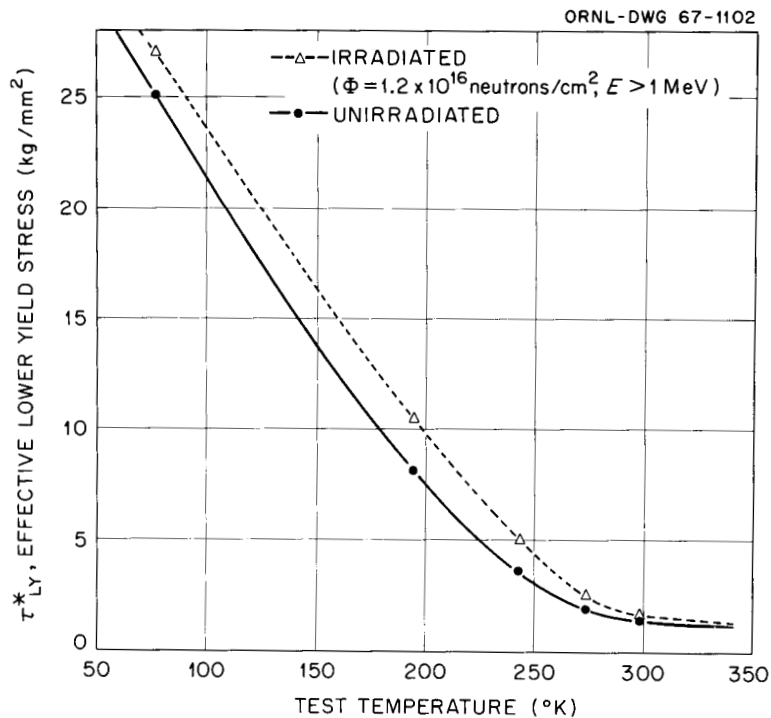


Fig. 11. Temperature Dependence of Effective Lower Yield Stress for Unirradiated and Neutron Irradiated Iron.

On the other hand, the activation volume is related to the following microscopic quantities,

$$v = b d \ell , \quad (2)$$

where b is the Burgers vector and d and ℓ are the size and the average spacing, respectively, of the barriers that give rise to the short range resistance to dislocation motion. In determining the activation volume, both the rate change test and the stress relaxation method are employed. In the rate change test, the increment in stress accompanying a sudden change in the cross-head speed is measured. In the stress relaxation method, the cross-head motion is halted and the subsequent decrease in stress is measured continuously as a function of time. It has been shown¹⁸ that the rate of stress relaxation is directly proportional to the plastic strain rate due to the motion of dislocations. It is, therefore, possible to measure the strain rate dependence of the applied stress from the analysis of the relaxation curve.

Figure 12 shows a plot of the activation volume as a function of the effective stress for both unirradiated and irradiated iron. It is found that data obtained by the two methods are in good agreement. It can be seen from the plot that, although there is an indication of a very slight increase in the activation volume particularly at high effective stresses, data from both unirradiated and irradiated samples fall along a single smooth curve. The results are also in good agreement with those obtained by Conrad¹⁴ for unirradiated iron. It may be stated that the effect of neutron irradiation is to raise the effective stress for deformation but when the activation volume is compared at the same level of effective stress there is no change due to irradiation. According to the definition of the activation volume, this behavior implies that the neutron irradiation does not introduce new barriers to dislocation motion, in addition to those that are already present in unirradiated crystals.

¹⁸G. M. Ohr, "A Study of Radiation Hardening in Iron by Stress Relaxation Techniques," p. 10.15 in Quarterly Progress Report: Irradiation Effects on Reactor Structural Materials, May-July 1965, Pacific Northwest Laboratory, Richland, Washington, BNWL-128, 1965.

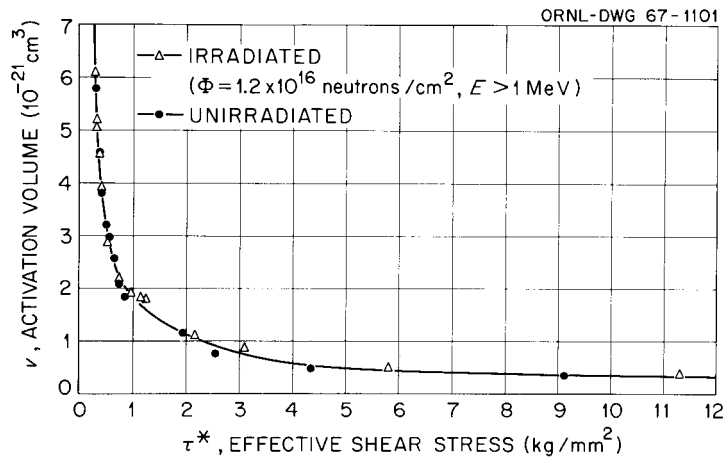


Fig. 12. Activation Volume vs Effective Shear Stress for Unirradiated and Neutron Irradiated Iron.

Another parameter of interest is the activation energy, H , associated with the thermal activation of dislocation motion. The activation energy is defined as

$$H = H_0 - v \tau^* , \quad (3)$$

where H_0 is the total activation energy, or the maximum interaction energy between the barriers and the moving dislocations. The second term on the right hand side, $v \tau^*$, corresponds to the work done by the applied stress during the thermal activation. The total activation energy, H_0 , is further defined as

$$H_0 = F_0 d/2 , \quad (4)$$

where F_0 is the maximum force required for a segment of dislocation to surmount a barrier of the diameter d . The activation energy, H , is determined experimentally through an expression¹³

$$H = - v T \left(\frac{\partial \tau}{\partial T} \right)_{\dot{\epsilon}} , \quad (5)$$

where $(\partial \tau / \partial T)_{\dot{\epsilon}}$ is the temperature dependence of the yield or flow stress.

Figure 13 shows a plot of the activation energy as a function of the effective stress. It shows that the activation energy is consistently higher after neutron irradiation. The values of the total activation energy, H_0 , may be estimated from Fig. 13 by extrapolating the curves to zero effective stress. The estimated values of H_0 are approximately 0.87 eV and 0.97 eV for unirradiated and irradiated crystals, respectively. The value of H_0 for unirradiated iron is somewhat higher than that previously given by Conrad.¹⁴ The discrepancy can be attributed to the method by which the effective stress is assigned. In Conrad's analysis, the effective stress was evaluated with respect to the stress at 300°K. This has an effect in underestimating the effective stress and hence the value of H_0 , since the activation energy increases rapidly as the effective stress approaches zero. The present data also yields a value for H_0 of approximately 0.7 eV at 300°K, in agreement with Conrad's data. From the preliminary nature of the present work, a question remains as to whether the observed increase in the activation energy upon irradiation is real. In order to establish the effect of irradiation on the activation energy, H_0 , more accurately, a more careful measurement of the temperature and strain rate dependence of the yield stress particularly in the low range of effective stresses is needed. This is the range that will greatly influence the value of

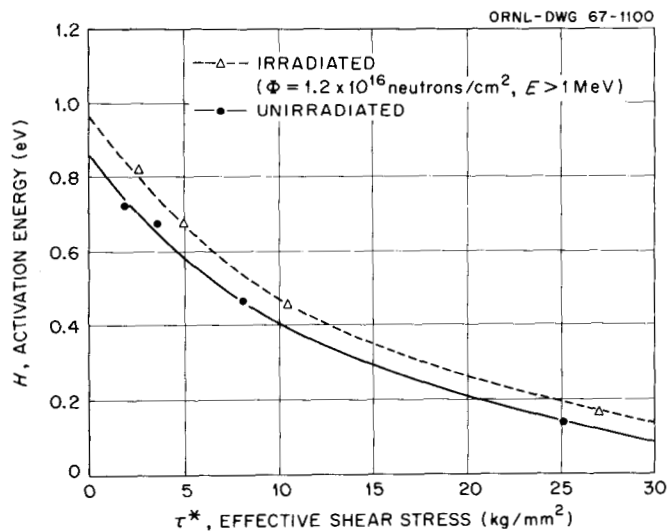


Fig. 13. Activation Energy vs Effective Shear Stress for Unirradiated and Neutron Irradiated Iron.

H_0 , but unfortunately the activation volume and the temperature dependence vary too rapidly to permit accurate determination.

Although an effort is being made to supplement these experimental data, it now appears that neutron irradiation does not seem to alter the size and density of barriers to dislocation motion in iron. It is recalled that even unirradiated iron exhibits a strong temperature dependence of yield stress. Therefore, it has been suggested that barriers present prior to neutron irradiation can interact strongly with moving dislocations. The defects introduced by irradiation are not sufficiently effective to interfere with dislocation motion as a new separate entity. The apparent increase in the activation energy implies that the irradiation induced defects merely strengthen the barriers that are already present in unirradiated crystals.

Niobium: Purification and Perfection *

R. E. Reed

This report will describe work which produced the purest niobium single crystals obtained in the Research Materials Program at ORNL during the past six months. An annealing treatment which resulted in niobium single crystals with good crystalline perfection will also be described.

A. Purification

Experimental Procedure

Niobium metal was obtained from the Parma Research Laboratory, Union Carbide Corporation, Parma, Ohio. It was in the form of electrodeposited metal cut from the edge of a cathodic plate deposit. In this case, the niobium metal was electrodeposited from a solution about 10 weight per cent NbF_5 in a mixture of alkali fluorides at a temperature of about $775^\circ C$ and a current density of about 50 ma/cm^2 with commercially pure niobium as anode material. ¹⁹

*Work sponsored by the Research Materials Program of the A.E.C.

¹⁹ G. W. Mellors and S. Senderoff, "Electrodeposition of Coherent Deposits of Refractory Metals: I. Niobium," J. Electrochem. Soc. 112, 266 (1965).

The metal was then electron beam drop cast into a water cooled copper mold with a 1/2-inch inside diameter. This casting was then cold swaged to 3/16-inch-diameter rod.

Table 2 lists the impurity levels of this material before and after the drop casting operation. The oxygen level was reduced from 200-300 ppm to 95 ppm. The hydrogen level was also lowered from 5-30 ppm to 1 ppm while the nitrogen content remained about the same. However, the carbon content increased from 1-6 ppm to 30 ppm. Also, there was an increase in the Ta and W content. Fe was reduced from 70 ppm to < 1 ppm during the drop casting operation. All other impurities were also less than 1 ppm after the drop casting operation.

Table 2
Impurity Analysis of Parma Niobium
After Various Melting Operations
In Weight Parts Per Million

Impurity	Electro-Deposited	Drop Cast	Zone Refined
C	1 - 6*	30	32
O	200 - 300*	95	3
N	5 - 10*	5	2
H	5 - 30*	1	1
Ta	5	18	19
W	1	14	15
Fe	70	< 1	< 1

*These values were taken from reference 19.

The 3/16-inch-diameter niobium rod was then electron-beam floating-zone refined in a bakeable stainless steel system which has been described in reference 20. The rod was given 10 zoning passes at a speed of 5.0 in/hr. The vacuum was 1×10^{-6} torr during much of the first pass but steadily improved until it attained 8×10^{-10} torr during the last two passes. The rod was a single crystal which was seeded such that the rod axis was near the center of the unit triangle. Table 2 lists the impurity analyses after this operation. The oxygen and nitrogen levels were 3 and 2 ppm respectively. The other impurities were relatively unchanged.

The resistance ratio of the rod was measured between room temperature and liquid hydrogen temperature and was found to be: $R_{300^\circ\text{K}}/R_{20^\circ\text{K}} = 256$. This ratio was also taken between room temperature and liquid helium temperature with the latter being done in a 12 K gauss magnetic field. This ratio was: $R_{300^\circ\text{K}}/R_{4.2^\circ\text{K}} (12 \text{ K gauss}) = 1420$.

A compression test was made on a specimen cut from the rod with a 3:1 length-to-diameter ratio. The ends were lapped flat and perpendicular to the rod axis. After a light chemical polish, this specimen was tested at a strain rate of $2.3 \times 10^{-4} \text{ sec}^{-1}$ on a table model Instron machine. The flow stress resolved on the $(\bar{1}01)[111]$ slip system was 900 gm/mm^2 .

Discussion

All pure niobium previously reported with $R_{300^\circ\text{K}}/R_{4.2^\circ\text{K}}$ (magnetic field) > 1000 has been prepared using a technique involving an anneal in high vacuum ($< 10^{-8}$ torr) at temperatures above 2200°C . Stromberg and Swenson²¹ and Fawcett, Reed, and Soden²² used this technique on wire type specimens to obtain resistance ratios of 1900 and 1600 respectively.

²⁰R. E. Reed, "Electron Beam Floating Zone Refining of Niobium," Proceedings of the Second International Conference on Electron and Ion Beam Science and Technology, April 17-20, 1966, New York, Gordon and Breach, to be published.

²¹T. F. Stromberg, and C. A. Swenson, "Negative Surface Free-Energy Effects in Superconducting Niobium," *Phys. Rev. Letters* **9**, 370 (1962).

²²E. Fawcett, W. A. Reed, and R. R. Soden, "High-Field Galvanomagnetic Properties of Ta and Nb," *Bull. Am. Phys. Soc.* **11**, 170 (1966).

Neither group reported any mechanical properties. However, Taylor and Christian²³ using the annealing procedure on 3mm-diameter single crystals of niobium reported a resolved yield stress in compression of 850 gm/mm² for a strain rate of 6×10^{-4} sec⁻¹. They also reported a resistance ratio of ~ 4000 for this material.

The niobium single crystals produced by electron beam-float-zone-refining from the Parma material at ORNL apparently approach the purity obtained by Taylor and Christian using their annealing technique. Further studies on this material involving high temperature anneals in high vacuum are in process.

B. Perfection

Experimental Procedure

A niobium single crystal seeded such that the rod axis was near a $\langle 211 \rangle$ crystallographic direction was grown using the electron-beam floating-zone technique. The niobium metal was obtained from Wah Chang Corporation. The effect of float-zone-refining upon the purity of this material has been previously described.²⁰ The 3/16-inch-diameter crystal was zoned one pass at 3.8 in/hr at $1-2 \times 10^{-6}$ torr vacuum.

A section 3/4-in.-long was cut from the rod using a high speed abrasive cut-off wheel. Parallel flats about 1/2-in.-long and 1.5mm apart were spark cut along the $[112]$ growth axis such that the $(\bar{1}10)$ plane was perpendicular to the flats. The flat surface was thus a $(11\bar{1})$ surface. After chemically polishing the specimen until the flats were 0.7mm apart, an anomalous transmission x-ray topograph (Borrmann topograph) was taken using molybdenum K_{α} radiation from $(\bar{1}10)$ reflection planes.

The specimen was then annealed for 2 hrs. 42 mins. at 2200°C in a 2×10^{-8} torr vacuum. R. F. induction heating was used. The specimen was placed in a 3/8-inch I.D. niobium susceptor which was inside a 1 1/4-inch-diameter tantalum split radiation shield. The 4-inch-diameter

²³G. Taylor, and J. W. Christian, "The Effect of High Vacuum Purification on the Mechanical Properties of Niobium Single Crystals," Acta Met. 13, 1216-1218 (1965).

induction coil was outside the 2 1/2-inch I.D. pyrex water cooled vacuum jacket which surrounded the work. The temperature was measured using an optical pyrometer sighted on one end of the specimen. After annealing, another Borrmann topograph was taken.

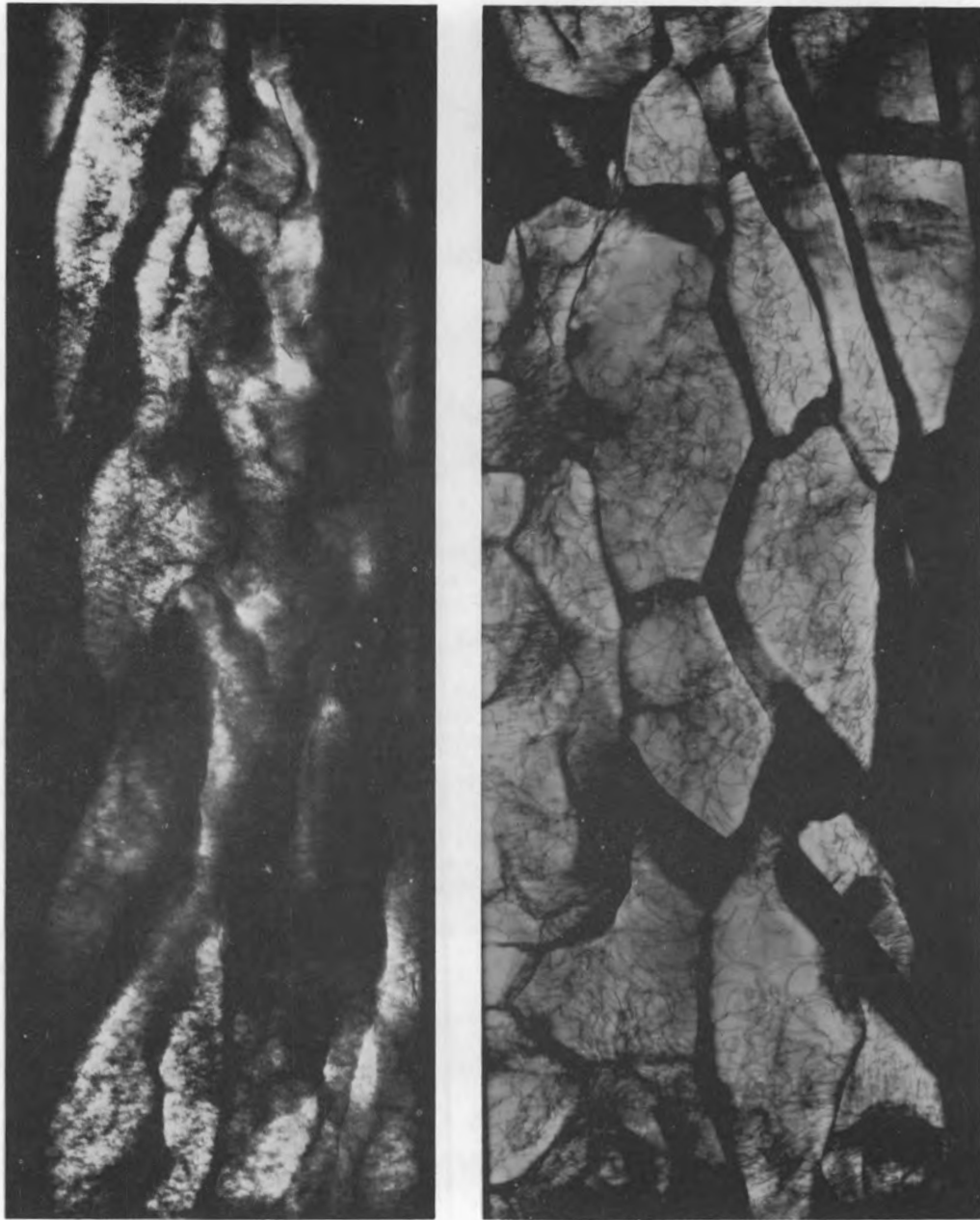
Discussion

Figure 14a is a Borrmann topograph showing the as-grown dislocation structure. The substructure consisted of sub-boundaries of less than 180 sec misorientation elongated in the growth direction. In addition, there were other areas showing rather dense tangles of dislocations.

Figure 14b is the same specimen after annealing. The subgrain boundaries have become very sharp compared to the as-grown condition. However, they still have a misorientation < 180 sec. The interiors of the subgrains have a low dislocation density which approaches 10^2 lines/cm². Anneals at 1800°C to 2000°C for times of about 2 hours did not result in any detectable change in the perfection of other similar specimens. Evidently, temperatures above 2200°C in a vacuum $< 10^{-8}$ torr are necessary to obtain appreciable changes in crystalline perfection for annealing times of a few hours. It may be significant that these same annealing conditions are those used by other investigators²¹⁻²³ to obtain resistance ratios ($R_{300^\circ\text{K}}/R_{4.2^\circ\text{K}}$ (magnetic field) > 1000 and resolved yield stresses below 1000 gm/mm². Fawcett, Reed, and Soden²² have noted that high values for the resistance ratio do not necessarily imply high chemical purity. It is suggested here that high crystalline perfection may be a factor in obtaining large resistance ratios for niobium in addition to high purity.

Conclusions

Niobium metal prepared by electrodeposition from a solution of NbF₅ in molten alkali metal fluorides was an excellent starting material for obtaining high purity niobium single crystals using electron-beam-floating-zone-refining. The low Ta and W contents were very important since the zone refining does not reduce the level of these impurities. A resistance ratio $R_{300^\circ\text{K}}/R_{4.2^\circ\text{K}}$ (12 K gauss) = 1420 and a resolved



(a) As-Grown (18X)

(b) Annealed (18X)

Fig. 14. Borrmann topographs using MoK_α radiation from the $(\bar{1}10)$ reflection of a niobium single crystal in (a) the as-grown condition and (b) after annealing at 2200°C for $2\frac{3}{4}$ hours at 2×10^{-8} torr vacuum.

shear stress for yielding in compression = 900 gm/mm^2 was obtained for this material after 10 float zone refining passes at 5 in./hr. in a final vacuum of 8×10^{-10} torr. The perfection of as-grown niobium single crystals can be improved by annealing 4 hours at temperatures above 2200°C in vacuums better than 5×10^{-8} torr.

Concerning the Etching of Dislocations in Niobium

H. D. Guberman

As has been demonstrated, etch pits may be produced in niobium which are associated with dislocations.²⁴ In all cases studied the dislocations associated with grown-in sub-boundaries and those randomly distributed throughout the sub-grain were easily etched. In addition, fresh dislocations introduced by either deforming through the yield point or stressing elastically near the yield point were also etched with apparent ease. Recently however, it became all but impossible to produce etch pits at new dislocations in the accustomed manner. Investigations indicate that the ability to etch dislocations in niobium is affected by the state of the material and in certain instances is directly associated with the presence of carbon at the dislocations.

All the samples studied were ostensibly identical. The earlier polycrystalline material and single crystals, which etched satisfactorily,²⁵ and the later single crystals, which etched poorly, were prepared from the same Wah Chang starting stock in the manner described by Reed.²⁶ The difference in the behavior of the material thus suggested that it had somehow been altered during preparation. This was corroborated by

²⁴H. D. Guberman, "Dislocation Etch Pits in Niobium," Radiation Metallurgy Section Solid State Division Progress Rept., Feb. 1966, ORNL-3949, p. 56

²⁵H. D. Guberman, "Dislocation Etch Pits in Niobium," Radiation Metallurgy Section Solid State Division Progress Rept., Aug. 1965, ORNL-3878, p. 49.

²⁶R. E. Reed, "High Vacuum Electron Beam Floating Zone Refiner," Radiation Metallurgy Section Solid State Division Progress Rept., Feb. 1966, ORNL-3949, p. 35.

observations on the superconducting properties of niobium single crystals prepared during the period in which the non-etching samples were grown. It was found that, compared to material grown earlier, the transition temperature decreased while the upper critical field at 4.2°K increased indicating an increase in the impurity content.²⁷ It was subsequently determined that the vacuum system in which the crystals were grown was operating at a higher pressure due to a fault; this could conceivably be the cause of the anomalous behavior though the precise nature of the contamination is not known.

This suggests that impurities play a significant role which was not apparent earlier. At about this time it became known that oxygen played no part in the etching but that carbon significantly enhanced dislocation etching in niobium.²⁸

This was immediately verified by depositing a flash coating of carbon in a vacuum onto a sample which had been indented and then aged at 1050°C for 10 1/2 hours. Prior to the carbon deposition and aging, the usual etching treatment did not show any new dislocations (Fig. 15), but afterwards showed them quite clearly (Fig. 16).

Aging temperatures substantially lower than 1000°C with or without carbon deposition, did not aid in etching dislocations. Annealing for 18 hours at 400°C or 16 hours at 600°C after carbon deposition did not significantly enhance the etching of fresh dislocations. However, in the first case, subsequent redeposition of carbon and aging at 1050°C for 11 hours revealed the pits clearly. In the second case, re-aging at 1025°C for 17 hours without prior carbon deposition did not reveal any but grown-in dislocations as before.

The above experiments are significant for two reasons. First, they establish that it is the carbon and not the aging treatment which is of primary importance in revealing the dislocation site by etching. Secondly, in the material at hand, it is not possible to cause a redistribution of carbon by low temperature aging as was done by Evans²⁹ to

²⁷S. T. Sekula, private communication.

²⁸R. Vardiman, Naval Research Laboratory, Washington, D. C., private communication.

²⁹P. R. V. Evans, "Dislocation Etch Pit Studies in Annealed and Deformed Polycrystalline Niobium," *J. Less-Common Metals* 6, 253 (1964).

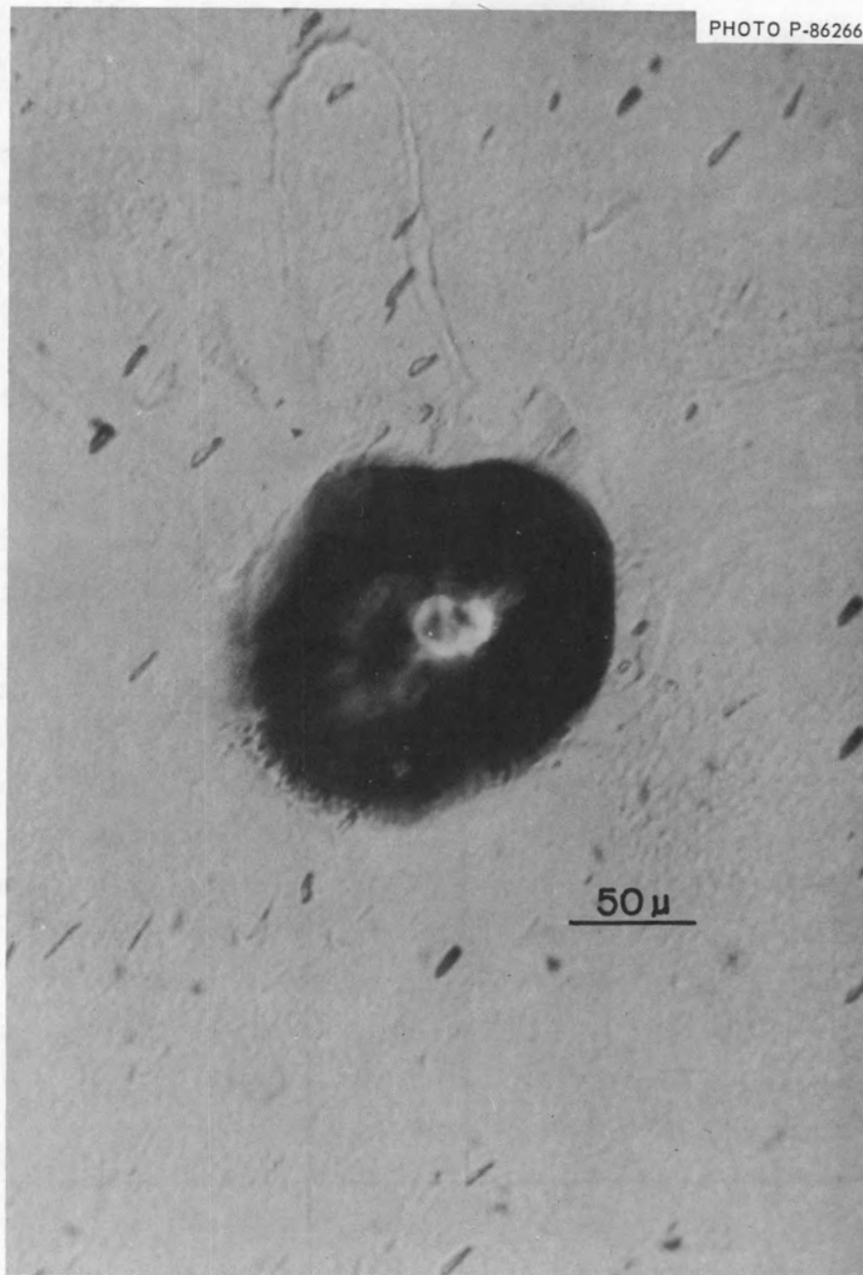


Fig. 15. Area Surrounding Indentation in a Nb Sample Shows Apparently no Fresh Dislocation Pits after Usual Etching Procedure.

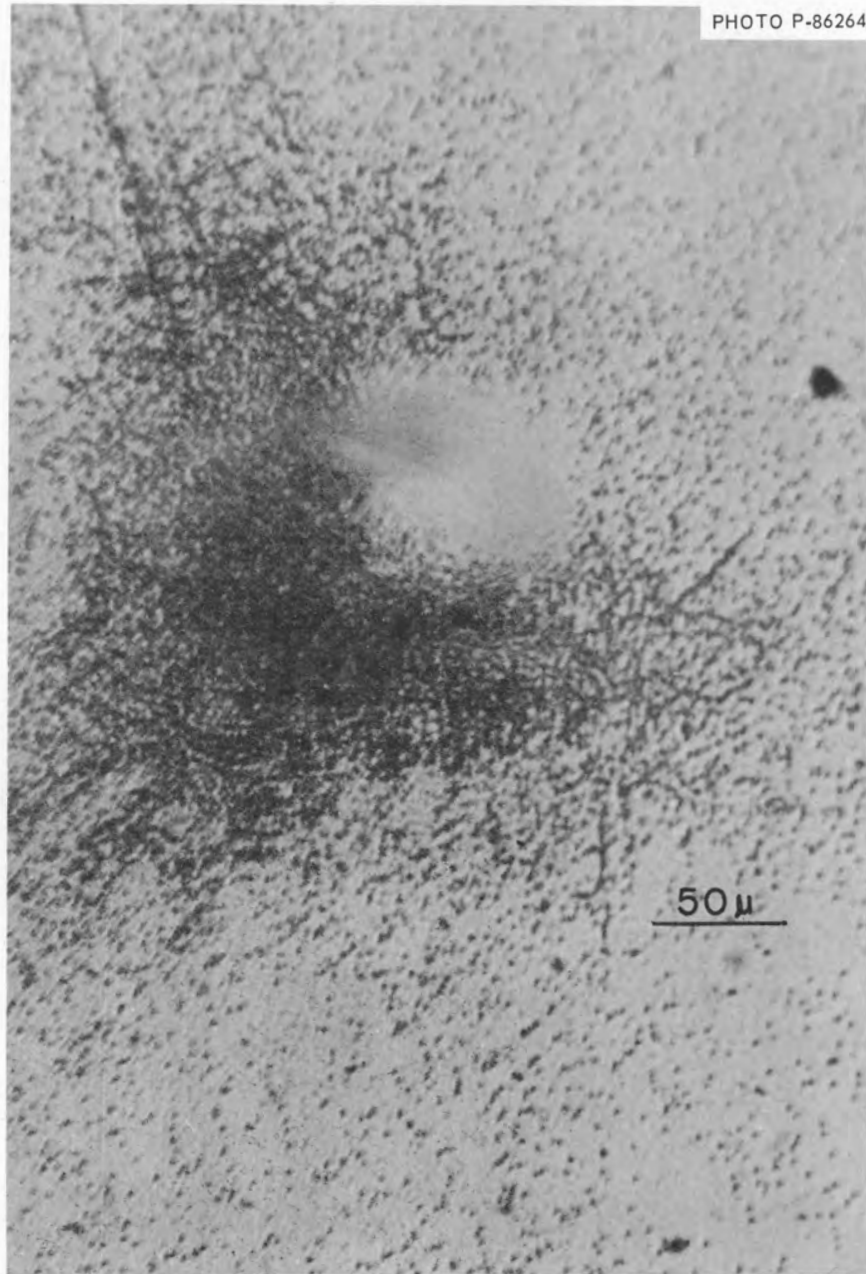


Fig. 16. Fresh Pits Associated with Deformation in the Vicinity of the Indentation were Easily Brought Out after a Flash Carbon Deposition and High Temperature Aging Treatment Prior to Chemical Etching.

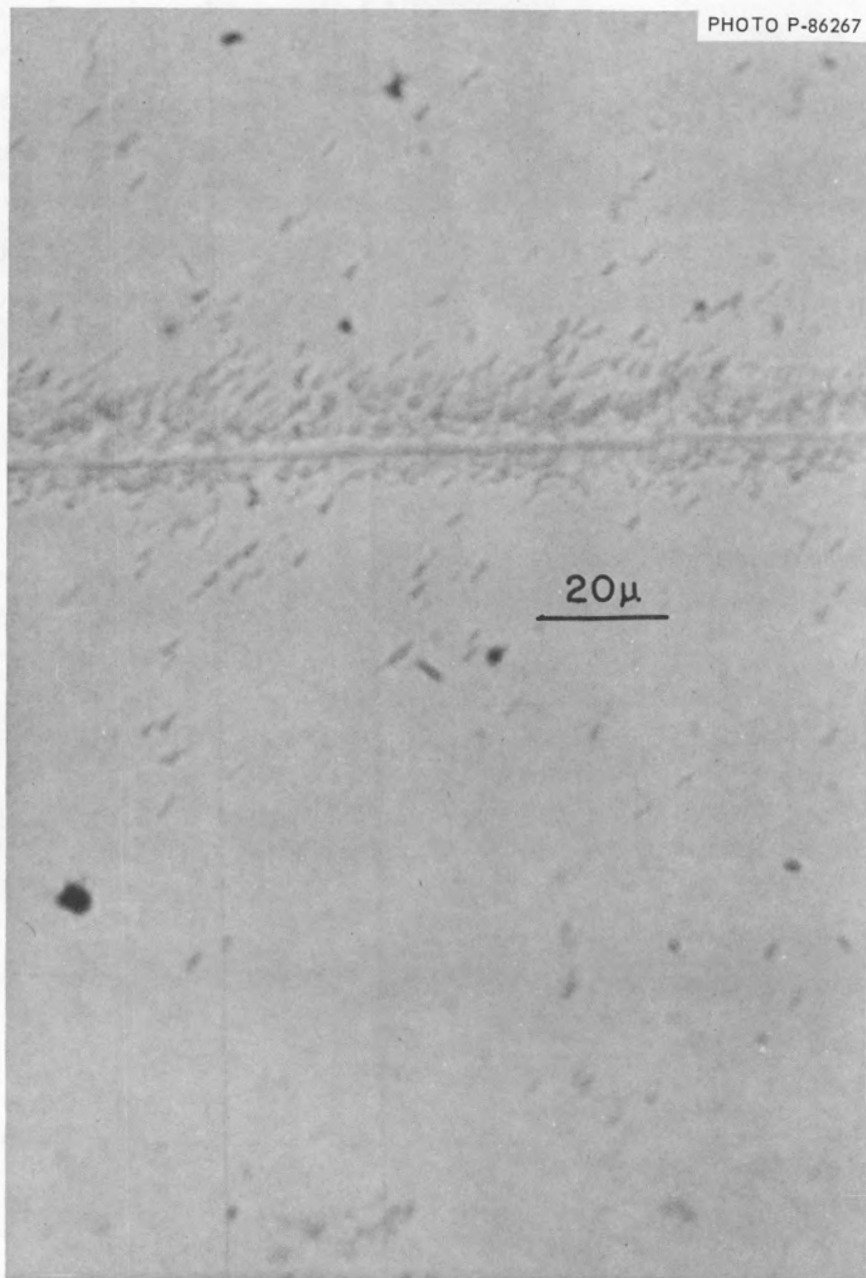


Fig. 17. Pits Along a Scratch in Nb Revealed by the Carbon Deposition Technique.

radiation hardening is produced by annealing in this range.³¹⁻³³ Annealing in this temperature interval is called Stage III annealing by most authors. Stage III annealing in b.c.c. metals has been attributed to either vacancy migration,³⁴ interstitial migration³⁵ or interstitial impurity migration.^{36,37} As pointed out in the previous report³⁸ we believe that Stage III annealing is due to interstitial impurity migration, and we presented evidence obtained from internal friction measurements to verify that oxygen atoms do migrate to irradiation produced defects in the temperature range of Stage III annealing. In this report additional evidence obtained from resistivity and internal friction measurements is presented to show that the Stage III annealing in niobium is caused by oxygen migrating to radiation produced defects.

Specimen Preparation

The samples used in these experiments were prepared by swaging and drawing zone refined niobium³⁹ rods to 0.030 inch diameter wire suitable for both internal friction and resistivity measurements. The wires were

³¹M. J. Makin and F. J. Minter, "The Mechanical Properties of Irradiated Niobium," *Acta Met.* 7, 361 (1959).

³²A. S. Wronski and A. A. Johnson, "A Hardening Effect Associated with Stage III Recovery in Neutron Irradiated Molybdenum," *Phil. Mag.* 8, 1067 (1963).

³³N. E. Hinkle, this report.

³⁴D. E. Peacock and A. A. Johnson, "Stage III Recovery in Neutron Irradiated Molybdenum and Niobium," *Phil. Mag.* 8, 563 (1963).

³⁵J. Nihoul, "The Recovery of Radiation Damage in Molybdenum," *Phys. Stat. Sol.* 2, (1962).

³⁶A. R. Rosenfield, "Recovery of Cold Worked Body Centered Cubic Metals," *Acta Met.* 12, 119 (1964).

³⁷F. Schlat and A. Kothe, "Einfluss des Sauerstoffgehalts auf die Erholung von Kalwerformtem Fantal," *Acta Met.* 14, 425 (1966).

³⁸J. T. Stanley and W. E. Brundage, "The Interaction of Radiation Produced Defects and Interstitial Impurity Atoms in Niobium," Radiation Metallurgy Section Solid State Division Progress Report for Period Ending July 1966, ORNL-4020, Sept. 1966, p. 49.

³⁹R. E. Reed, "Electron Beam Floating Zone Refining of Niobium," Proceedings of the Second International Conference on Electron and Ion Beam Science and Technology, Gordon and Breach Publishers, New York, April 17-20, 1966. To be published.

then annealed and outgassed at various temperatures ranging from 1800 to 2200°C by resistive heating in vacua ranging from 5×10^{-6} to 3×10^{-9} torr. These treatments resulted in samples with various concentrations of the three principal interstitial impurities, C, O, and N. Since the purpose of these experiments is to focus attention on the role of oxygen in the radiation annealing, an attempt was made to add oxygen to two of the samples, D and F, following the original outgassing treatment. This was done by reheating the samples to a temperature lower than the outgassing temperature in an atmosphere of O_2 . For sample F the resulting oxygen concentration was ~ 260 ppm by weight. However, for sample D the conditions necessary for adding oxygen were not achieved and some carbon was inadvertently added instead.

The interstitial impurity levels of these specimens were characterized by means of internal friction and resistivity measurements. The data of Powers and Doyle⁴⁰ provide a quantitative correlation between internal friction peak heights and concentration for O and N. The resistivity contribution of oxygen was taken as $0.0039 \mu\Omega\text{-cm/wt ppm}^{41}$ ($6.7 \mu\Omega\text{-cm/at } \%$) and that of nitrogen was $0.005 \mu\Omega\text{-cm/wt ppm}$ ($10 \mu\Omega\text{-cm/at } \%$)⁴². Neither the damping effect nor the resistivity of carbon is known, but estimates of the carbon concentration were obtained under the assumption that the values for O and N are at least representative of those for carbon. Attempts to measure carbon concentration were further limited by the fact that carbon has a very low solubility at low temperatures. Thus, some of the carbon may precipitate out during cooling and any carbon retained in solution rapidly precipitates during the time required for making internal friction measurements.

⁴⁰R. W. Powers and Margaret V. Doyle, "Diffusion of Interstitial Solutes in the Group V Transition Metals," *J. Appl. Phys.* 30, 514 (1957).

⁴¹C. S. Tedmon, Jr., R. M. Rose, and J. Wulff, "Controlled Addition of Small Amounts of Oxygen to Niobium (Columbium)," *Trans. AIME* 230, 1732 (1964).

⁴²R. A. Pasternak and B. Evans, "The Effect of Dissolved Nitrogen on the Electrical Resistance of Niobium (Columbium)," *Trans. AIME* 233, 1194 (1965).

In general, the total interstitial impurity concentrations predicted from the resistivity data were in good agreement with those obtained from internal friction measurements. These methods and some preliminary measurements will be presented in more detail later, but a summary of the annealing information, resulting impurity concentration and resistivity data are given in Table 3.

The principal metallic impurities are Ta and W. The concentration of these impurities depends only on the source of the pre-zoned starting material, since zoning has no effect on their concentrations.³⁹ Material from two sources was used in these experiments and the appropriate levels of Ta and W are also indicated in Table 3.

Measurement Techniques

A description of the internal friction equipment and procedures has been given in a previous report.³⁸ For purposes of resistivity measurements, primary potential contacts of 0.010 in. diameter Nb wire were spot-welded to the samples. These contacts remained with the samples throughout the preliminary measurements, irradiation, and subsequent isochronal annealing to be described later. Thus, the gage length was constant for a given sample over the course of its entire series of treatments. The accuracy of the absolute resistivity values given is limited to about $\pm 4\%$ by our knowledge of the sample geometry. Platinum wire contacts were spotwelded to the primary niobium contacts and copper leads were attached to the Pt by soldering. The resistance measurements were made by the potentiometer technique using a Rubicon Six Dial Microvolt Potentiometer. The sample was immersed in liquid helium inside a superconducting magnet capable of 20 kilogauss. The resistance values were picked off the superconducting transition curve at fields ranging from 15 to 18 kilogauss, as required to insure that each sample was fully normal.

Pre-Irradiation Measurements

Internal friction measurements on sample A are shown in Fig. 18. The difference between the first and second run data shown is due to the precipitation of carbon during the first run measurements. Internal friction measurements on samples C and E are shown in Fig. 19. In both of these

Table 3. Annealing Temperatures, Vacua, and Resulting Characteristics for Niobium Samples.

Sample	Annealing Temp. (°C)	Final Vacuum Achieved During Annealing	Re-Heating Temp. (°C)	Re-Heating atm	Resistivity ($\mu\Omega$ -cm) at 4.2°K	$R_{\text{Room Temp.}}$	Interstitial Impurities Weight ppm	Metallic Impurities
						$R_{4.2^\circ\text{K}}$		
A	1800	5×10^{-6} torr	--	--	--	--	40 (O) 60 (C) 7.7 (N)	367 Ta 227 W
B	1700	5×10^{-6}	--	--	--	--	70 (O) 60 (C) 12 (N)	367 Ta 229 W
C	2100	1×10^{-7}	--	--	0.069	208	< 3 (O) 3 (C) 10 (N)	367 Ta 227 W
D	2100	1×10^{-7}	1700	5×10^{-8} torr (O ₂)	0.27	57	< 3 (O) 30 (C) 10 (N)	367 Ta 227 W
E	2200	3×10^{-9}	--	--	0.017	870	< 4 (O) < 4 (C) < 4 (N)	367 Ta 227 W
F	2200	5×10^{-9}	1100	5×10^{-6}	1.0	16	260 (O)	296 Ta 73 W

specimens the oxygen peak seems to be buried in the background damping and is certainly less than 1×10^{-4} . This value of internal friction corresponds to about 3 ppm by weight of oxygen. The resistivity of sample E ($0.017 \mu\Omega\text{-cm}$) would correspond to about 4 ppm oxygen if the total resistivity were attributable to oxygen. However, the large metallic impurity concentration probably accounts for much of this resistivity, so that the oxygen content should be much less. Nitrogen and carbon remain in sample C in sufficient quantities to produce the small peaks shown in Fig. 19 and the observed resistivity of $0.069 \mu\Omega\text{-cm}$. Both specimens show decreases in the background damping at temperatures where the oxygen atoms become mobile. This effect is especially pronounced in sample E.

The internal friction measurements on sample F are shown in Fig. 20. The oxygen peak height of 75×10^{-4} corresponds to 260 ppm of oxygen. The resistivity of $1.0 \mu\Omega\text{-cm}$ corresponds to ~ 255 ppm.

Irradiation and Annealing Procedures

Internal friction specimens from samples A and B were irradiated to doses of 8×10^{17} and 1.6×10^{18} ($E > 1.0$ Mev) respectively in position P-5 of the Bulk Shielding Reactor. The irradiation temperature was 50°C .

Resistivity and internal friction specimens from samples C, D, E, and F were irradiated in position C-41 of the LIIR. Samples C and D were irradiated together to a dose of approximately 1×10^{18} neutrons/cm² ($E > 1.0$ Mev) and E and F were irradiated simultaneously to a dose of 2×10^{18} neutrons/cm² ($E > 1.0$ Mev). The irradiation temperature was $\sim 50^\circ\text{C}$ for both irradiations.

Post irradiation annealing of the internal friction specimens was done in conjunction with the internal friction measurements. The resistivity specimens were isochronally annealed for periods of 1 hr. at 25°C temperature intervals starting with 75°C . The annealing was done with the samples in a quartz tube attached to a UHV pumping system. A tube furnace was preheated to the desired annealing temperature and placed around the tube. The pressure in the vacuum system during these anneals never exceeded 1×10^{-7} torr.

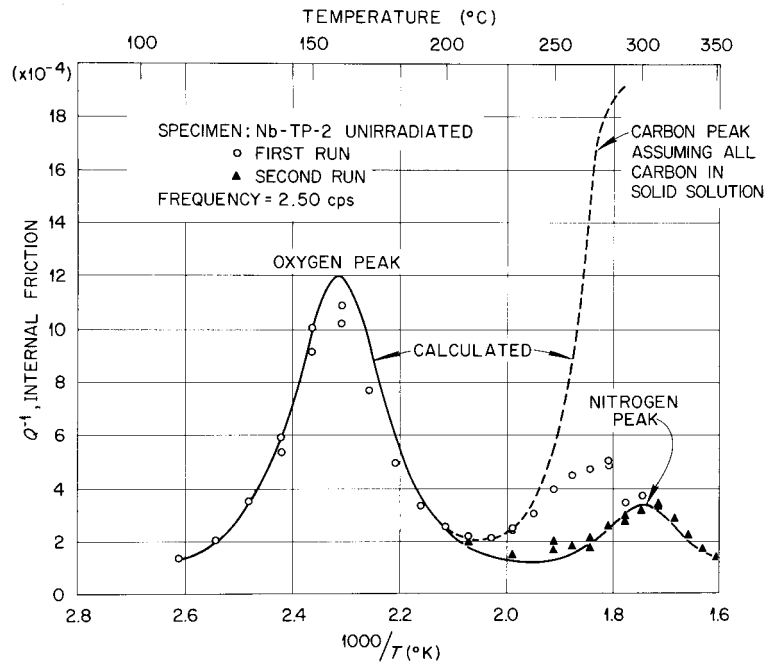


Fig. 18. Pre-Irradiation Internal Friction Measurements on Sample A.

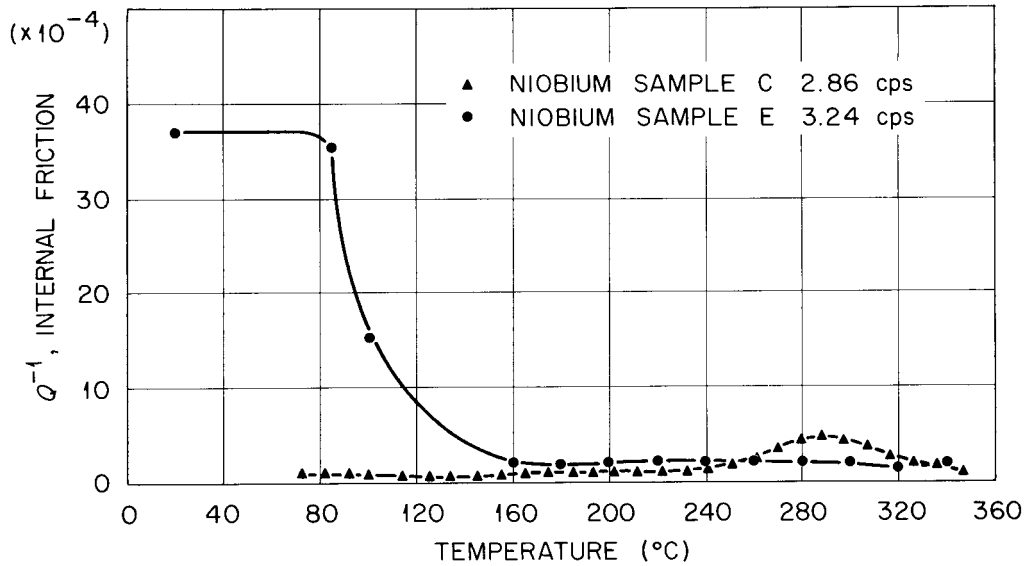


Fig. 19. Pre-Irradiation Internal Friction Measurements on Samples C and E.

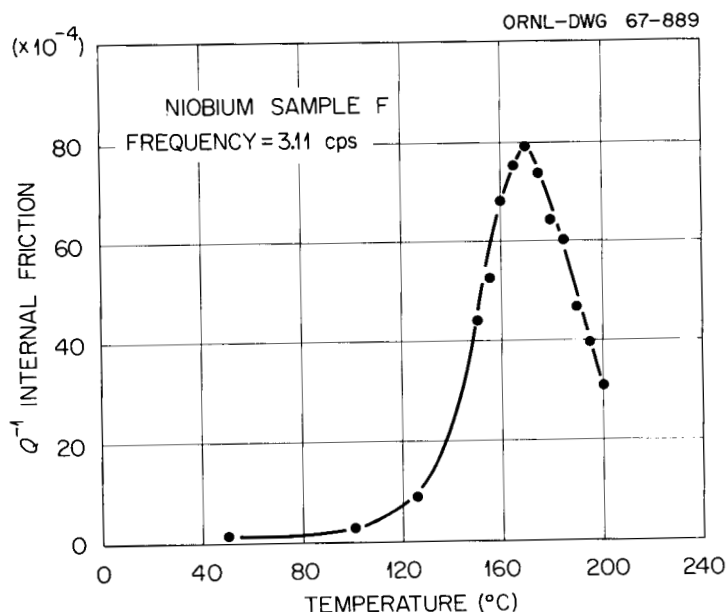


Fig. 20. Pre-Irradiation Internal Friction Measurements over the Oxygen Peak Region in Sample F.

Internal Friction Results

Internal friction measurements on specimen A were reported previously.³⁸ Internal friction measurements on specimen B were made as a function of time at the oxygen peak temperature in order to determine the decrease of the peak with time. The results are shown in Fig. 21. Internal friction measurements on specimens from irradiated samples C, D, E, and F showed no changes from the pre-irradiated measurements.

Resistivity Results

Figure 22 shows the post irradiation isochronal annealing data for samples C and D. The change in resistivity is taken with respect to the pre-irradiation value. Thus, we see that sample D, the more impure sample, increased about twice as much as sample C for this dose. The annealing results on sample C appear somewhat erratic but no marked annealing stages appear up to 325°C. At 325°C the sample appears to be approaching its pre-irradiation value. It is planned to extend these anneals to 400°C.

Sample D exhibits a sharp decrease in resistivity setting in above 200°C. The resistivity goes well below the pre-irradiation value. As was previously mentioned, carbon precipitation occurs in this temperature

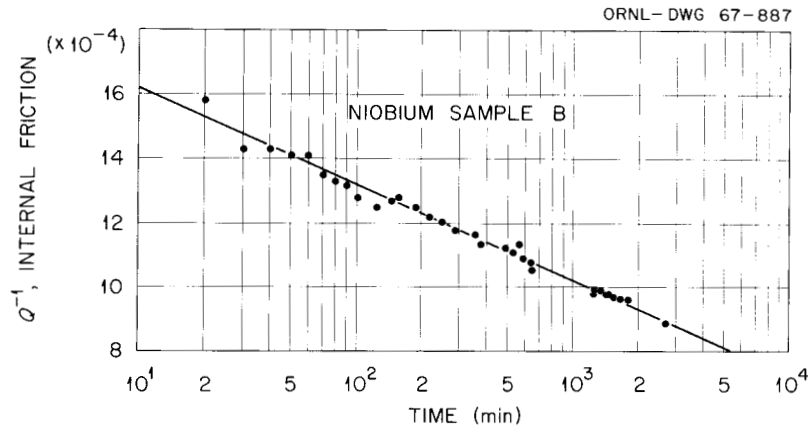


Fig. 21. Decrease in Oxygen Peak Height versus Time at the Peak Temperature (150°C) for Sample B Irradiated to 1.6×10^{18} neutrons/cm² ($E > 1.0$ Mev). Frequency = 0.854 cps. $Q^{-1}(t = 0) = 19.5 \times 10^{-4}$.

region, even in unirradiated samples.³⁸ We therefore feel that this annealing stage is probably not related to radiation effects. In order to test this contention, annealing of control (unirradiated) specimens of both C and D has been undertaken, but this annealing has not yet progressed beyond 200°C.

Significantly, neither sample exhibits an annealing stage in the vicinity of 125°C. The annealing stage obtained by Peacock and Johnson³⁷ for their dose of $\sim 1 \times 10^{19}$ ($E > \text{thermal}$) is also shown in Fig. 22. This dose should be comparable to our dose of $\sim 1 \times 10^{18}$ ($E > 1.0$ Mev). The curve of Peacock and Johnson³⁷ is arbitrarily placed along the ordinate so that their post-irradiation change in resistivity corresponds to that of sample D. Peacock and Johnson estimate their impurity concentrations at 500 ppm O, 50 ppm N, and 100 ppm C.

Figure 23 shows the annealing results obtained thus far on sample E and F. Again the irradiation produced a smaller resistivity increase in the purer sample (E) than in the contaminated sample (F). However, neither of these samples exhibited as large an increase as did either of the two previous samples (C and D) even though they were irradiated to a slightly larger dose. Sample F (260 ppm O) shows an annealing stage in the proper place for Stage III. Indeed, the resistivity goes below the pre-irradiation value. Little effect is observed in sample E or the two control specimens.

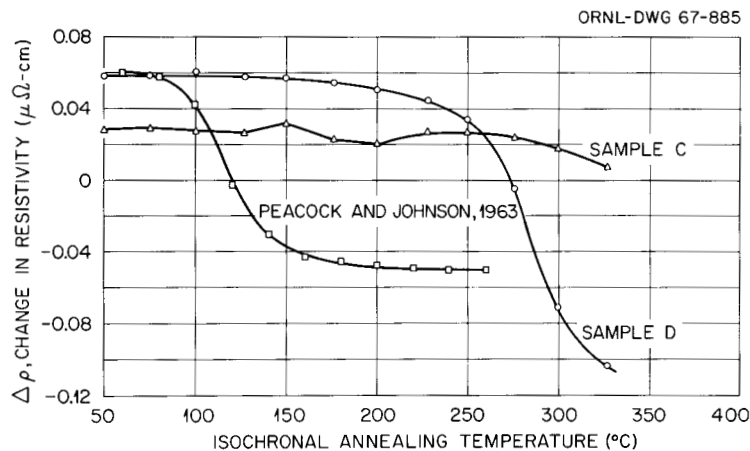


Fig. 22. Change in Resistivity versus Isochronal Annealing Temperature for Samples C and D after Irradiation to 1×10^{18} neutrons/cm² ($E > 1.0$ Mev) and for Commercial Niobium (500 ppm oxygen) after Irradiation to 1×10^{19} neutrons/cm² (epithermal).^{3,4}

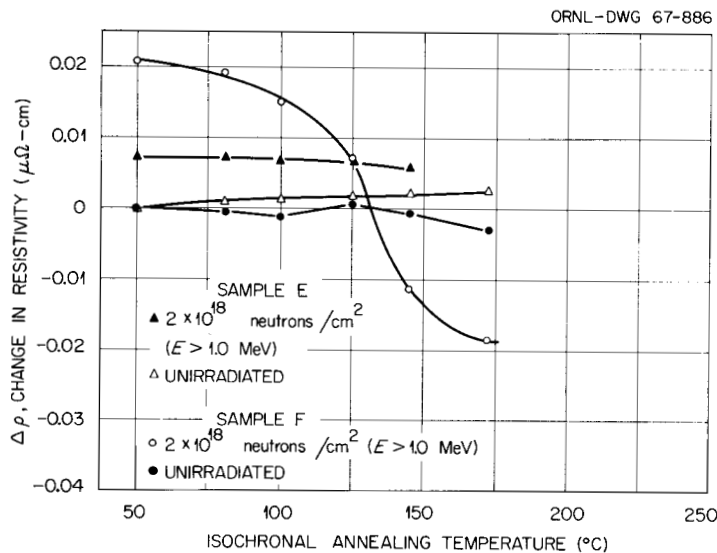


Fig. 23. Isochronal Annealing of Irradiated and Unirradiated Niobium Samples.

Discussion

This work has shown the following results: (1) In the temperature range of Stage III annealing in niobium no resistivity decrease of irradiated specimens is observed in the absence of interstitial impurity atoms. (2) If oxygen is present in irradiated niobium a resistivity decrease is observed upon annealing in the temperature interval from 75°C

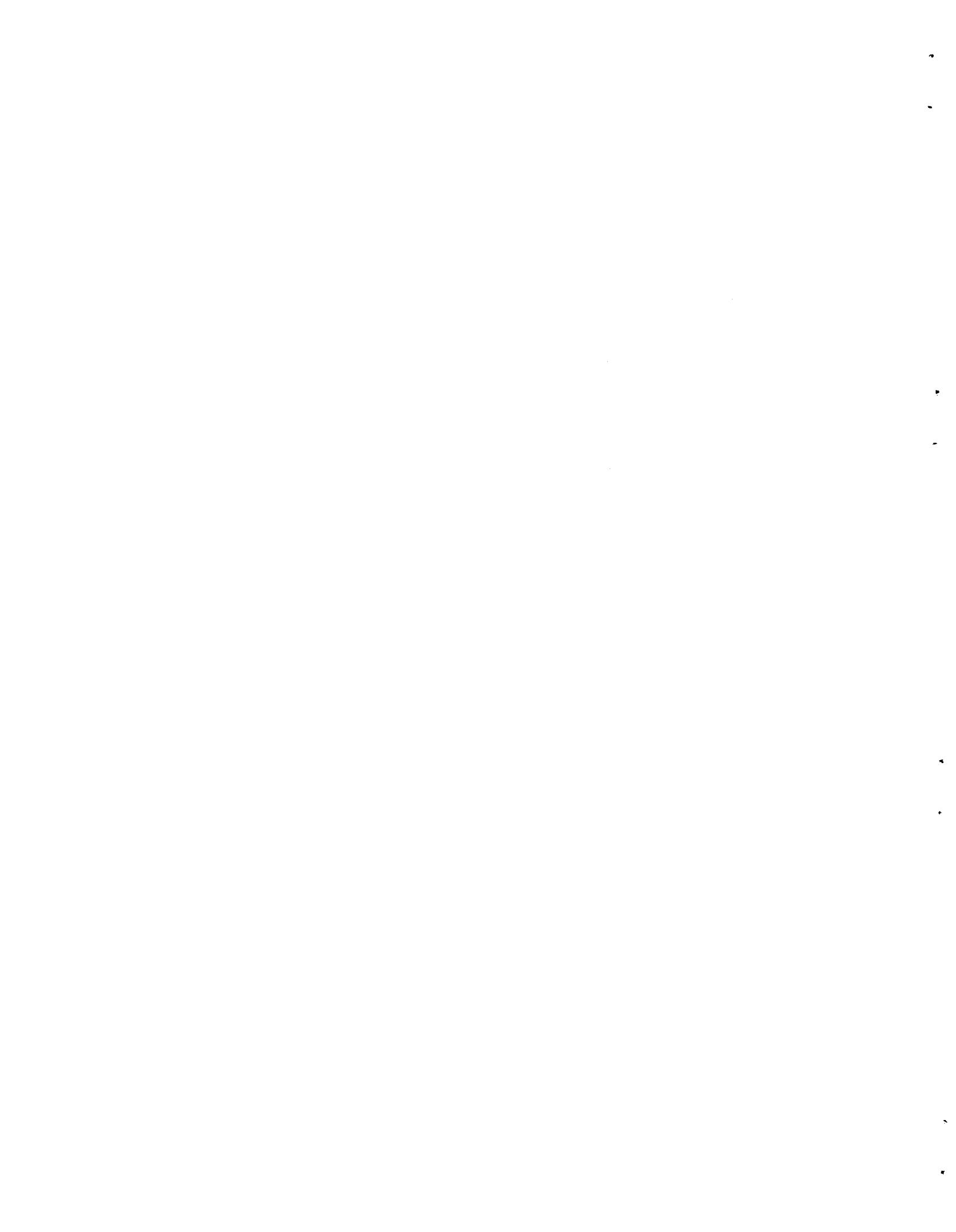
to 200°C. (3) If carbon is present in niobium a resistivity decrease is observed in the temperature interval 200 to 320°C. (4) The oxygen internal friction peak decreases after irradiation and annealing in the temperature interval near 150°C. From these facts we conclude that the resistivity decrease observed by Peacock and Johnson and the yield stress increase observed by Makin and Minter in this temperature range were caused by migration of oxygen atoms to irradiation produced defects.

We also observed that the initial purity and/or crystal perfection influences the amount of damage produced by the irradiation at 50°C and also the amount of annealing in Stage III. This suggests that the oxygen atoms migrate to a defect structure that was formed by migration of an elementary defect at some lower temperature and that the clusters of these elementary defects were nucleated by impurity atoms.

Stage III annealing has also been reported in other b.c.c. metals, and we are interested in speculating about the possibility that interstitial impurity atoms are responsible for the annealing Stage III in these other metals. Tungsten is particularly interesting since Kuhlmann and Schultz recently reported that neutron irradiated tungsten that had been degassed in high vacuum so as to remove interstitial impurities still showed Stage III annealing.⁴³ The estimate of interstitial content in their sample was based on resistivity at 4.5°K after rapid cooling from 1600°C. However, the solubility of interstitial impurities in tungsten is known to be very low at low temperature and at 1600°C most of the interstitial impurities are probably already precipitated as oxides and carbides.⁴⁴ We have previously shown evidence that carbon that has precipitated from solution in niobium can be put back into solution by neutron irradiation.³⁸ We suggest that this effect could account for the above mentioned observations in tungsten.

⁴³ H. H. Kuhlmann and H. Schultz, "Erholungsstufe III in Entkohltem Wolfram nach Neutronenbestrahlung bei 4.5°K," *Acta Met.* 14, 798 (1966).

⁴⁴ R. H. Schnitzel, "Internal Friction of Tungsten Single Crystals," *Trans. AIME* 233, 186 (1965).



INTERNAL DISTRIBUTION

- | | |
|-------------------------------------|--------------------------------------|
| 1-3. Central Research Library | 70. W. D. Compton (consultant) |
| 4-5. ORNL - Y-12 Technical Library | 71. T. F. Connolly |
| Document Reference Section | 72. J. H. Coobs |
| 6-25. Laboratory Records Department | 73. J. A. Cox |
| 26. Laboratory Records, ORNL R.C. | 74. J. H. Crawford, Jr. (consultant) |
| 27. ORNL Patent Office | 75. J. C. Crump |
| 28. M. M. Abraham | 76. F. L. Culler |
| 29. G. M. Adamson, Jr. | 77. J. E. Cunningham |
| 30. L. G. Alexander | 78. G. V. Czjzek |
| 31. R. W. Armstrong (consultant) | 79. P. B. DeNee |
| 32. W. E. Atkinson | 80. J. H. DeVan |
| 33. Robert Bakish (consultant) | 81. D. A. Douglas, Jr. |
| 34. T. O. Baldwin | 82. Z. El Saffar |
| 35. J. H. Barrett | 83. J. H. Erwin |
| 36. S. E. Beall | 84. G. W. Glack |
| 37. R. J. Beaver | 85. J. L. Fowler |
| 38. P. R. Bell | 86. A. P. Fraas |
| 39. M. Bender | 87. J. H. Frye, Jr. |
| 40. W. T. Berg | 88. J. L. Gabbard |
| 41. R. G. Berggren | 89. W. B. Gauster |
| 42. Carla Bertocci (consultant) | 90. H. A. Gersch (consultant) |
| 43. U. Bertocci | 91. G. Gilat |
| 44. J. O. Betterton, Jr. | 92. J. H. Gillette |
| 45-46. D. S. Billington | 93. J. J. Gilman (consultant) |
| 47. H. Birnbaum (consultant) | 94. R. J. Gray |
| 48. A. L. Boch | 95. W. R. Grimes |
| 49. E. G. Bohlmann | 96. H. D. Guberman |
| 50. E. S. Bomar | 97. J. P. Hammond |
| 51. B. S. Borie | 98. W. O. Harms |
| 52. C. J. Borkowski | 99. C. S. Harrill |
| 53. G. E. Boyd | 100. M. R. Hill |
| 54. M. A. Breazeale (consultant) | 101. N. E. Hinkle |
| 55. M. A. Bredig | 102. D. K. Holmes |
| 56. R. B. Briggs | 103. A. S. Householder |
| 57. F. R. Bruce | 104. J. P. Howe (consultant) |
| 58. W. E. Brundage | 105. J. T. Howe |
| 59. C. T. Butler | 106. A. P. Huber (K-25) |
| 60. N. Cabrera (consultant) | 107. L. D. Hulett |
| 61. J. W. Cable | 108. H. Inouye |
| 62. J. V. Cathcart | 109. L. H. Jenkins |
| 63. Y. Chen | 110. R. J. Jones |
| 64. R. O. Chester | 111. W. H. Jordan |
| 65. H. R. Child | 112. G. W. Keilholtz |
| 66. G. W. Clark | 113. B. C. Kelley |
| 67. J. W. Cleland | 114. M. T. Kelley |
| 68. A. M. Clogston (consultant) | 115. R. H. Kernohan |
| 69. R. R. Coltman | 116. R. F. Kimball |

117. E. M. King
118. C. E. Klabunde
119. F. A. Kocur
120. J. S. Koehler (consultant)
121. W. C. Koehler
122. R. B. Korsmeyer
123. J. A. Krumhansl (consultant)
124. J. A. Lane
125. C. E. Larson
126. G. Leibfried (consultant)
127. A. B. Lewis
128. R. S. Livingston
129. A. L. Lotts
130. T. S. Lundy
131. H. G. MacPherson
132. G. Mazzone
133. R. W. McClung
134. H. C. McCurdy
135. D. L. McElroy
136. C. J. McHargue
137. A. Meyer
138. A. J. Miller
139. E. C. Miller
140. J. W. Mitchell (consultant)
141. H. A. Mook
142. R. M. Moon, Jr.
143. K. Z. Morgan
144. C. M. Nelson (consultant)
145. R. M. Nicklow
146. T. S. Noggle
147. A. S. Nowick (consultant)
148. O. S. Oen
149. S. M. Ohr
150. A. R. Olsen
151. V. Pare
152. P. Patriarca
153. M. L. Picklesimer
154. J. C. Pigg
155. H. Pomerance
156. J. W. Prados
157. L. J. Raubenheimer
158. J. K. Redman
159. R. E. Reed
160. C. C. Robinson
161. M. T. Robinson
162. J. R. Russell
163. H. W. Savage
164. O. E. Schow
165. J. L. Scott
166. S. T. Sekula
167. F. A. Sherrill
168. E. D. Shipley
169. W. A. Sibley
170. R. H. Silsbee (consultant)
171. O. Sisman
172. G. M. Slaughter
173. L. Slifkin
174. G. P. Smith
175. H. G. Smith
176. A. H. Snell
177. E. Sonder
178. A. L. Southern
179. F. Specht
180. J. T. Stanley
181. J. O. Stiegler
182. W. J. Stelzman
183. B. G. Streetman
184. A. Taboada
185. E. H. Taylor
186. L. C. Templeton
187. A. S. Tetelman (consultant)
188. G. T. Trammell (consultant)
189. D. B. Trauger
190. R. P. Tucker
191. David Turnbull (consultant)
192. H. A. Ullmaier
193. D. Walton
194. C. C. Webster
195-295. M. S. Wechsler
296. R. A. Weeks
297. A. M. Weinberg
298. J. R. Weir, Jr.
299. R. D. Westbrook
300. G. D. Whitman
301. E. P. Wigner (consultant)
302. M. K. Wilkinson
303. F. E. Williams (consultant)
304. G. C. Williams
305. J. M. Williams
306. R. O. Williams
307. W. R. Willis (consultant)
308. J. C. Wilson
309. M. C. Wittels
310. E. O. Wollan
311. R. F. Wood
312. J. R. Woodyard
313. H. L. Yakel
314. F. W. Young
315. Gale Young
316. W. H. Young

EXTERNAL DISTRIBUTION

317. C. M. Adams, Jr., Massachusetts Institute of Technology
318. S. Amelinckx, Solid State Physics Department, C.E.N., Mol-Donk, Belgium
319. P. Baruch, Laboratoire de Physique, Ecole Normale Supérieure, Paris V, France
320. V. B. Bhanot, Physics Department, Panjab University, Chandigarh-3, India
321. T. H. Blewitt, Argonne National Laboratory
322. Boeing Airplane Company
323. R. O. Bolt, California Research Corporation, Richmond
324. J. A. Brinkman, North American Aviation Science Center, Thousand Oaks, California
325. H. Brooks, Harvard University, Cambridge, Massachusetts
326. R. B. Burlin, Atomic Energy Commission, Washington
327. J. G. Castle, Jr., Physics Department, Westinghouse Electric Corporation, Research Laboratories, Pittsburgh, Pennsylvania
328. R. A. Charpie, Union Carbide Corporation, New York
329. E. D. Clavert, U.S. Bureau of Mines, P. O. Box 492, Albany, Oregon
330. C. B. Cooper, Department of Physics, University of Delaware, Newark, Delaware
- 331-332. D. F. Cope, RDT Site Office (Oak Ridge National Laboratory)
333. D. Dautreppe, CEN-B, Boite Postale No. 269, Grenoble, France
334. J. Diehl, Max Planck Institut für Metallforschung, Seestrasse 75, Stuttgart N, Germany
335. H. D. Dietze, Lehrstuhl für Reaktorwerkstoffe, Technische Hochschule, Aachen, Germany
336. J. F. Elliott, Massachusetts Institute of Technology
337. L. B. Emlet, Union Carbide Corporation, New York
338. N. Engel, Georgia Institute of Technology
339. H. Y. Fan, Solid State Physics Department, Purdue University, Lafayette, Indiana
340. H. B. Finger, Atomic Energy Commission, Washington
341. J. D. Fleming, Georgia Institute of Technology
342. V. D. Frechette, Alfred University
343. J. Friedel, Physique des Solides, Faculté des Sciences d'Orsay, Orsay, France
344. Angelo Giambusso, Atomic Energy Commission, Washington
345. R. G. Gilliland, Massachusetts Institute of Technology
346. R. H. Gillette, European Research Associates, Brussels, Belgium
347. J. L. Gregg, Bard Hall, Cornell University
348. W. W. Grigorieff, Assistant to the Executive Director, Oak Ridge Associated Universities
349. R. F. Hehmann, Case Institute of Technology
350. J. Hitch, Office of Isotope Development, AEC, Washington
351. E. E. Hoffman, General Electric, Cincinnati, Ohio
352. H. Huntington, Department of Physics, Rensselaer Polytechnic Institute, Troy, New York
353. J. R. Johnson, Minnesota Mining and Manufacturing Company, St. Paul, Minnesota

354. L. K. Keys, General Electric, Cincinnati, Ohio
355. C. Kikuchi, University of Michigan, Willow Run Laboratory, Ann Arbor, Michigan
356. O. C. Kopp, University of Tennessee, Knoxville
357. J. Korringa, Ohio State University
- 358-359. W. J. Larkin, Atomic Energy Commission, Oak Ridge
360. Benjamin Lax, Lincoln Laboratory, Lexington, Massachusetts
361. C. Lehmann, KFA-Werkstoffinstitut, Julich, Germany
362. R. I. Leininger, Battelle Memorial Institute, Columbus, Ohio
363. A. B. Lidiard, AERE, Harwell, England
364. J. J. Lombardo, NASA, Lewis Research Center
365. W. M. Lomer, AERE, Harwell, England
366. W. C. Mallard, Emory University, Atlanta, Georgia
367. W. D. Manly, Union Carbide Corporation, Stellite Division
368. W. Marshall, AERE, Harwell, England
369. R. S. Mateer, University of Kentucky
370. P. W. McDaniel, Division of Research, USAEC, Washington
371. A. Merlini, Solid State Physics Department, C.C.R.-EURATOM, Ispra (Varese), Italy
372. R. M. Milton, Linde Division, Union Carbide Corporation, P. O. Box 44, Tonawanda, New York
373. Peter Murray, AERE, Harwell, England
374. R. R. Nash, NASA, Washington
375. E. F. Nippes, Rensselaer Polytechnic Institute
376. H. M. Otte, Martin Company, Orlando, Florida
377. R. E. Pahler, Atomic Energy Commission, Washington
378. R. M. Parke, MAB, National Academy of Science, Washington
379. J. Pheline, Centre d'Etudes Nucleaires de Saclay
380. J. M. Prosser, Atomic Energy Commission, Washington
381. H. B. Rahner, Savannah River Operations
382. R. E. Reed-Hill, University of Florida
383. Research and Development Division, AEC, ORO
384. F. N. Rhines, University of Florida
385. A. E. Ruark, Atomic Energy Commission, Washington
386. H. Saito, Department of Physics, College of General Education, Osaka University, Osaka, Japan
387. A. F. Saturno, University of Tennessee, Knoxville
388. R. W. Schroeder, NASA, Lewis Research Center
389. R. J. Schuttler, Service SEPP, CEN/FAR (Ford de Chatillion), Boite Postale 6, Fontenay-aux-Roses (Seine), France
390. F. C. Schwenk, Atomic Energy Commission, Washington
391. A. Seeger, Max Planck Institut fur Metallforschung, Seestrasse 75, Stuttgart N, Germany
392. F. Seitz, University of Illinois, Urbana, Illinois
393. W. W. Shaver, Corning Glass Works, Corning, New York
394. A. A. Shoudy, Atomic Power Development Associate, Inc.
395. J. M. Simmons, Division of Reactor Development, AEC, Washington
396. O. C. Simpson, Argonne National Laboratory
397. E. E. Sinclair, Atomic Energy Commission, Washington
398. A. Sosin, Atomics International, Canoga Park, California
399. E. E. Stansbury, University of Tennessee, Knoxville
400. D. K. Stevens, Materials and Metallurgy Branch, AEC, Washington

401. G. L. Stiehl, Convair Division of General Dynamics Corporation, San Diego, California
402. R. Street, Department of Physics, Monash University, P. O. Box 92, Clayton, Victoria, Australia
403. J. A. Swartout, 270 Park Avenue, New York 17, New York
404. D. O. Thompson, North American Aviation Science Center, Thousand Oaks, California
405. J. B. Trice, Military Space Vehicle Department, General Electric Company, Philadelphia, Pennsylvania
406. T. J. Turner, Department of Physics, Wake Forest College, Winston-Salem, North Carolina
407. A. Van Echo, Atomic Energy Commission, Washington
408. G. H. Vineyard, Brookhaven National Laboratory, Upton, Long Island, New York
409. J. B. Wagner, Massachusetts Institute of Technology
410. G. D. Watkins, General Electric Research Laboratories, Schenectady, New York
411. Watt Webb, Union Carbide Metals
412. J. Weertman, Northwestern University
413. G. W. Wench, Atomic Energy Commission, Washington
414. Westinghouse Electric Corporation, Research Laboratories, Pittsburgh, Pennsylvania
415. M. J. Whitman, Atomic Energy Commission, Washington
416. C. H. T. Wilkins, University of Alabama
417. Manfred Wuttig, University of Missouri, Rolla, Missouri
418. C. D. Yost, ARPA, Pentagon, Washington, D.C.
419. R. A. Young, Georgia Institute of Technology, Atlanta, Georgia
- 420-691. Given distribution as shown in TID-4500 under Metals, Ceramics, and Materials category (25 copies - CFSTI)